Impact of fuel additives on the performance, combustion and emission characteristics of diesel engine charged by waste plastic bio-diesel

Jayashri N. Nair [a], T. Nagadurga [b], V. Dhana Raju [c,**], Harish Venu [d], Sameer Algburi [e], Sarfaraz Kamangar [f], Amir Ibrahim Ali Arabi [f], Abdul Razak [g,*], Narasimha Marakala [h]

[a] *Department of Mechanical Engineering, VNR Vignana Jyothi Institute of Engineering and Technology, Hyderabad, 500090, Telangana, India*
[b] *Department of Electrical and Electronics Engineering, Malla Reddy Engineering College, Medchal, 500100, Secunderabad Telangana, India*
[c] *Department of Mechanical Engineering, Lakireddy Bali Reddy College of Engineering, Mylavaram, 521230, AP, India*
[d] *Centre of Research Impact and Outcome, Chitkara University, Rajpura, 140417, Punjab, India*
[e] *Al-Kitab University, Kirkuk, Iraq*
[f] *Mechanical Engineering Department, College of Engineering, King Khalid University, Abha, 61421, Saudi Arabia*
[g] *Department of Mechanical Engineering, P. A. College of Engineering (Affiliated to Visvesvaraya Technological University, Belagavi), Mangaluru, 574153, India*
[h] *Nitte (Deemed to be University), NMAM Institute of Technology, Nitte, Karkala, Karnataka, 574110, India*

ARTICLE INFO

ABSTRACT

Plastic waste in the environment has increased rapidly in recent years, amounting to nearly 4 million metric tons per annum globally. This waste comprises materials such as low-density polyethylene, high-density polyethylene, polyethylene terephthalate, polystyrene, and more. The current research focuses on the use of plastic waste as a biofuel for diesel engines. The properties of waste plastic oil blended fuels were calibrated to meet ASTM standards. Various blended mixtures of waste plastic biofuels were prepared and labelled as WPO10, WPO20, and WPO30. These mixtures were tested in a diesel engine under standard conditions. Based on the initial results, the optimized blend was further examined with fuel additives, such as the alcohol additive 1-butanol and alumina oxide nanoparticles, at lower concentrations. This was done to evaluate the engine's performance, combustion, and emission characteristics. The addition of 5 % 1-butanol reduced CO and HC emissions by 9 % and 18.6 %, respectively, compared to WPOME20. Similarly, the inclusion of 100 ppm of Al_2O_3 nanoparticles decreased CO and HC emissions by 12.5 % and 18.5 %, respectively, compared to WPOME20. Further, the application of RSM-ML approach, the various characteristics of diesel engine is optimized further the WPO20 operated with 1-Butanol and Al_2O_3 nanoparticles.

* Corresponding author.
** Corresponding author.
E-mail addresses: jayashri@vnrvjiet.in (J.N. Nair), durga.269@gmail.com (T. Nagadurga), dhanaraju1984@gmail.com (V.D. Raju), harishvenuresearch@gmail.com (H. Venu), sameer.algburi@uoalkitab.edu.iq (S. Algburi), aarabi@kku.edu.sa (S. Kamangar), sarfaraz. kamangar@gmail.com (A.I. Ali Arabi), arkmech9@gmail.com (A. Razak), nmarakala@nitte.edu.in (N. Marakala).

Abbreviations:

BTE	Brake thermal efficiency	WPO 20 1-Butanol 5 %	5 % addition of 1-Butanol to WPO 20
BSFC	Brake specific fuel consumption	WPO 20 1-Butanol 10 %	10 % addition of 1-Butanol to WPO 20
CO	Carbon monoxide	WPO 20 Al_2O_3 50ppm	50 ppm of Al_2O_3 addition to WPO 20
HC	Hydrocarbons	WPO 20 Al_2O_3 100ppm	100 ppm of Al_2O_3 addition to WPO 20
NOx	Nitrogen oxides	RSM	Response Surface Methodology
SO	Smoke Opacity	ML	Machine Learning
WPO	Waste plastic oil	GBR	Gradient Boosting Regression
WPO 10	10 % waste plastic oil +90 % Diesel	RF	Random Forest
WPO 20	20 % waste plastic oil +80 % Diesel	DT	Decision Tree
WPO 30	30 % waste plastic oil +70 % Diesel	ANOVA	Analysis of Variance

1. Introduction

Plastic is a kind of flexible and synthetic substance so easily mould into various shapes. It is formed by various organic polymers like polyethylene, nylon etc. Plastic is strong and deteriorates gradually because of chemical linkages that also make it resistant to deterioration caused by natural processes. Plastics can be classified into two sorts; those are thermosets and thermoplastics. When heated, a thermoset solidifies or "sets" permanently. Because of their strength and other favorable properties, these can be used in various applications like automotive and construction applications etc. Polyethylene, Polypropylene, Polyamide, Poly-oxymethylene, and Poly Tetra-fluoro-ethylene are examples of these plastics. When heated, a thermoplastic softens, and when it cools to room temperature, it resumes its original shape. It is simple to shape and mould thermoplastics into items like milk jugs etc. With the growth in the population of global and the growing need for food and additional necessities, there has been a spike in the quantity of waste being produced everyday by every home, as per to new statistics, plastics may remain unmodified up to 4500 years on climate [1]. Nearly 5 % of municipal solid trash is discovered to be harmful plastic in various forms. Frequently, in everywhere plastic things like empty bags are appeared. Due to its biodegradability, it causes water to stagnate and the resulting hygienic issues. Experiments have been conducted to determine whether this waste plastic may be utilized profitably to contain this issue.

Plastics are not created equal. There are numerous varieties of plastic in addition to a wide range of colors and shapes. Each one is unique and serves a particular purpose. Because of the chemicals they contain, some forms of plastic, like some that can be recycled, are reusable while others must be disposed of in a different way. Today, we'll go through the seven various varieties of plastic to help you make better judgments about the items you purchase. The various types of plastic materials are presented in Fig. 1.

Biodiesel made from various ways is currently more feasible than solar and wind power for immediate energy needs, as it can be easily produced, stored, and used in existing engines without the need for extensive infrastructure or weather-dependent conditions [3, 4]. Numerous researchers have investigated biodiesel at varying concentrations to evaluate its performance and emission characteristics [5,6]. Prabhu [7] Performed test on diesel engine with nanoparticles additive and Jatropha blended fuel. This work concluded that BTE improved 12 % with the aid of nanoparticles also HC, CO and smoke was reduced by 44 % 60 % and 38 % correspondingly for B20A30C30 when compared with B100. Jeryrajkumar et al. [8] analyzed the performance and discharge parameters engine charged with calophyllum bio-fuel. This work identified that the Colphyllum inophyllim bio-fuel (B100) containing closer kinematic viscosity and heating value hen associated with diesel. The HC with the additive of cobalt oxide indicated 80 % drop at peak conditions. Titanium dioxide gave that 70 % drop in 75 % load. And the BSFC was reduced in the nano-additives blends. Dhana Raju and Harish Venu [9] performed the experiment on influences of Zr2O3 additive in jatropha blended mixture at several loads. In that they concluded the B20 + 20ppm Zr2O3 blended mixture gave in 70.90 % greater BTE and 4.870 % dropped BSFC associated to B20, also COs, HCs, opacity and NOx discharges stood lesser than B20 by 11.360 %, 5.870 %, 6.871 %, and 9.563 %, correspondingly, when peak conditions. Swamy et al. [10] performed the test with tamarind seed oil blends at several proportions of butanol like 5 %, 10 % and 15 %. In that result they concluded that 5 % butanol biodiesel has revealed 3.21 % improvement in BTE when likened to TSME 20 at peak

Fig. 1. Different types of plastic [2].

conditions. Also, the BSFC for the TSME 20 + 5 % butanol was smaller value when associated to remaining mixtures of butanol. It was shown that 2.01 % drop in BSFC for the TSME 20 + 5 % butanol blended mixture when related to the TSME 20.

Prabhu and Anand [11] investigated on influence of Alumina and Cerium oxide nanoparticles as additive in jatropha bio-oil and observed 5 % development in BTE for test oils. Mohan et al. [12] Performed test on engine charged with nanoparticles added bio-fuel blended mixtures and understood that HP of bio-oil was 10–20 % greater related to diesel. Bio-fuel-CNG at 20 % formed higher torque related to remaining combinations. Bio-fuel sufficiently increased the CO (15–32 %) and nitric oxides (6.67–7.03 %) but reduced the HC (5.76–6.25 %) and CO (0.47–0.58 %) discharges range. Abbulfatah Abdu Yusuf et al. [13] explored on the impact of waste plastic oil, with Al_2O_3 and TiO_2 additives on engine when study-state mode. Observed that the WPO contained 64.25 % of alkanes which are noticeable amount which 28 % aromatics. Compared to EFs of EC, which approximately reduced 89.470 % across the Hy40 fuels. The decrease of ECs thru total blended combinations might be endorsed because of the increased in Al_2O_3 and TiO_2 proportions. Sajith et al. [14] experimentally investigated upon the impact of the mixing of cerium oxide with biodiesel. Found that the flash-point of bio-fuel, it was a sign of volatility was increased with the aid of the additive and the viscidness of the bio-oil was observed to be increased with cerium oxide. Which was also observed that cerium oxide helped in reduction of NO_X. Dhana Raju et al. [15] Performed test with diesel, MSME10, MSME20 and MSME30 at varying applications of load. They found that among those blended combinations MSME20 displayed well performance, emission and combustion possessions. Test result revealed that 200ppm mixing of Al_2O_3 to the MSME20 has given substantial augment of 1.390 % BTE and significant drops of HC and CO discharges by 35.480 % and 13.10 % respectively at peak conditions.

JaiKumar et al. [16] Studied about the analysis of burning, vibration, and noise features of engine charged with methyl ester of Mesua Ferra oil (MFOME) blended mixtures. The blended mixtures were B10, B20, and B40. They executed test on IPs of 180 bar, 200 bar and 220 bar. They found that at greater IPs of 220 bar, the CP, NIRR, CHRR and RoPR were enriched by 4.981 %, 9.233 %, 5.45 %, and 11.580 % correspondingly while the R.M.S velocity and R.M.S noise were decreased by 14.76 % and 3.54 % correspondingly for B20. Junshuai et al. [17] researched on added nano-additives CuO, Al_2O_3, MWCNT, CeO_2, GO, CNT, TiO_2, to diesel-bio-oil blended mixtures and had attained extraordinary fallouts. By means of engine performance, CeO_2 was the superior influence in reduced BSFC by a minor as 30 % and MWCNT was the improved BTE by 36.810 %. By means of discharge, TiO_2 had better outcome in decreasing of NO_x by 22.570 %, GNPs had the better impact in falling CO, with a decrement of 65.10 %, GO had the good effect in reduced HCs, with a decrement of 70 %.

Maneesh et al. [18] explored the production of crude oil from water hyacinth biomass and its conversion into biodiesel. To enhance fuel performance, the alcohol additive n-pentanol was blended with the biodiesel. Their experimental findings showed that for the WHB20D75P5 blend at maximum load, the brake-specific BSFC decreased to 0.26 kg/kW-h, and BTE increased by reached 29.5 %. There was reduction in emissions. Ahmad et al. (2016) directed an investigation on an engine charged by adding ethanol to diesel. In this experiment ethanol was mixed to diesel with 2 %, 4 %, 6 %, 8 %, 10 % and 12 %. The attained outcomes displayed torque and power augmented by 3.8 % blend with 6 % ethanol as related to diesel. Sarthak et al. [19] Researched on hydrogen diesel fueled with hydrogen to know combustion, vibration, and noise analysis. In this experiment 25 % 50 % and 75 % of loads of hydrogen. The obtained results were, decrease of vibration and noise level. Vibrations were increased due to active participate of hydrogen in the combustion, but this obtained at higher loads. Dueso et al. [20] directed test on engine fueled sunflower biodiesel with antioxidant additive. It can be detailed that substantial variances in amid of bio-fuel of sunflower seed and the same biodiesel mixed additive. Outcomes were concluded that instead of conventional fuels, this bio-oil with additive can be utilized.

Sathish Kumar Nagaraj et al. [21] investigated on emissions in engine by biofuel combined neem and pongamia using 3-hole and 4-hole nozzle. NO_x rises by rising the load, 3-hole nozzle discharges was identified that poorer with 4-hole nozzle. Ultimately, four-hole nozzles were suggested for engines for required needs to protect the climate from the gases. Gad et al. [22] executed a test on an engine performance, emissions and combustion features by carbon nanoparticles. The biodiesel extracted from waste cooking oil enhanced by carbon nanotubes. The blended mixture of biodiesel B20 mixed with different ranges of CNT and graphene nano-sheets. The results showed that BTE for B20CNT100 and B20CNS100 were 8 and 19 % about B20. Biofuel with CNT and graphene nanosheets of 100ppm attained considerable decrease in opacity by 28 % and 52 % respectively. Manoj Kumar et al. [23] inspected the impact of TiO_2 nano-additive on performance and emission features of engine fueled with Karanja biodiesel blend. In this experiment Karanja oil was added with anhydrous methanol and KOH as catalyst at 65 °C. Outcomes revealed that increased of BSFC to 7.14 %–10.71 %, increased of BTE to 1.72 %, abatement of COs and HCs and rise of NO_x were the outcomes from it. Jayaraman, J., & Reddy, S [24] accompanied a test on effect of IP on performance & emission features with graphene oxide additive in bio-oil blend. Sapota seed oil were used as biodiesel. The outcomes where NOx emissions for entire blends were lowered than diesel at high load of B10GO50 and higher emission than pure biodiesel. Gavhane and Kate [25] examined the impact of soybean biodiesel (SB)–diesel blends containing 1 % strontium-doped zinc oxide (Sr/ZnO) nanoparticles on the performance and emissions of a VCR engine. A 25 % soybean biodiesel blend (SB25) was enhanced with Sr/ZnO nanoparticles at concentrations of 50 and 75 ppm, using ultrasonication and a surfactant for stability. They found that the addition of 50 ppm Sr/ZnO to SB25 significantly improved engine performance, increasing BTE by 10.37 % and reducing BSFC by 16.76 %. Mourad et al. [26] directed a test on an engine for augmenting the performance and emission appearances. By employment of exhaust gas recirculation (EGR) and pre heated biodiesel on anl engine with a percentage was decreased to 25 % of EGR and preheated biodiesel. There was a clear reduction of emitted gases by using these biofuels. Rastogi et al. [27] assessed the performance of an engine characteristics and emission parameters using jojoba biodiesel blend (JB20). The nano-particles of CuO were added at 25, 50 and 75ppm into the JB20 fuel. The results shown that BTE for JB20CN50 oil was greater than remaining jojoba bio-fuel blends. Emissions of engine HCs, COs and opacity discharges were observed lower when CuO nano-particles mingled to JB20 and at peak load NOx were enlarged by 0.4, 0.7, 1.8 % for JB20CN50, JB20CN50 and JB20CN75 fuels correspondingly.

Mitchell et al. [28] studied the engine -bowl with oxygenated fuel at cold and hot conditions and the authors found better lubricity and lower viscosity of oxygenated fuels enhanced the performance of diesel engine during cold start operation. Hossain et al.[29] [] [] [] examined the microalgae HTL fuel effects on diesel engine performance and exhaust emissions using surrogate fuels and they revealed that Major emissions including PM, PN and CO were reduced significantly with increasing of NOx emission. Hedayat et al. [30] presented about the oxygen content of few biodiesels on particulate oxidative potential and they noticed that increase in ROS production, the oxygen content of the fuel also increased.

From the detailed review of existing literature, it is evident that waste plastic oil can be effectively extracted from plastic waste and utilized in diesel engine applications. Furthermore, blending waste plastic oil with fuel additives has demonstrated significant improvements in engine performance, including enhanced efficiency and reduced exhaust emissions.

This experimental research investigates the impact of using 1-Butanol and alumina oxide (Al_2O_3) as fuel additives in a blend containing 20 % waste plastic fuel. The study evaluates the performance, combustion, and emission characteristics of this blend under varying load conditions. This combination capitalizes on the high calorific value of waste plastic fuel (WPF), the oxygenation properties of 1-Butanol to enhance combustion efficiency, and the catalytic properties of Al_2O_3 nanoparticles to achieve cleaner combustion and minimize pollutant formation. As an oxygenated fuel, 1-butanol improves the oxygen availability during combustion, leading to better fuel-air mixing and more complete combustion. This reduces the formation of pollutants like carbon monoxide and unburned hydrocarbons. Additionally, 1-butanol has a higher energy density and miscibility with hydrocarbons, making it compatible with WPO while improving engine performance and stability. Its renewable nature also supports sustainability goals in alternative fuel applications.

In addition, the application of Response Surface Methodology (RSM) integrated with machine learning (ML) introduces a novel approach to optimizing key engine parameters, such as brake thermal efficiency, fuel consumption, and emissions. By combining experimental data with advanced computational techniques, this study provides a robust, predictive framework for achieving sustainable and efficient diesel engine performance. The findings pave the way for environmentally friendly fuel alternatives and contribute to addressing global challenges in energy sustainability and emission reduction.

2. Materials and methods

Waste plastic, a major environmental challenge due to its non-biodegradability and widespread availability, can be effectively managed through pyrolysis, a process that converts it into waste plastic oil (WPO), a hydrocarbon-rich fuel alternative to diesel. To optimize engine performance and emissions using such alternative fuels, Response Surface Methodology (RSM) and Machine Learning (ML) play a crucial role. RSM designs experiments evaluates factor interactions, while ML provides predictive models for optimizing parameters like brake thermal efficiency, fuel consumption, and emissions, ensuring efficient and sustainable fuel utilization.

2.1. Pyrolysis of waste plastic oil

Pyrolysis is defined as thermal degradation of plastic at superior temperatures and in an inert atmosphere. Which is an irreversible process and plastics transformed to hydrocarbon particles. The usage of the pyrolysis method is that it can be applied to convert wasted plastic into valuable oils.

The layout of pyrolysis setup is shown in Fig. 2. The oil formed through the pyrolysis method has a superior heating value and can be applied as substitute fuel. So, wasted plastic can be heated in pyrolysis with the absence of oxygen to form an oil. For transportation oils, which can be purified if required further. Its suitability as a good alternate fuel because it's extensive properties. The various fuel properties of diesel and waste plastic oil blends are presented in Table 1.

An economic analysis for waste plastic oil (WPO) to this study will provide insight into the feasibility and benefits of using it as a biofuel alternative. The economic analysis of WPO is presented in Table 2.
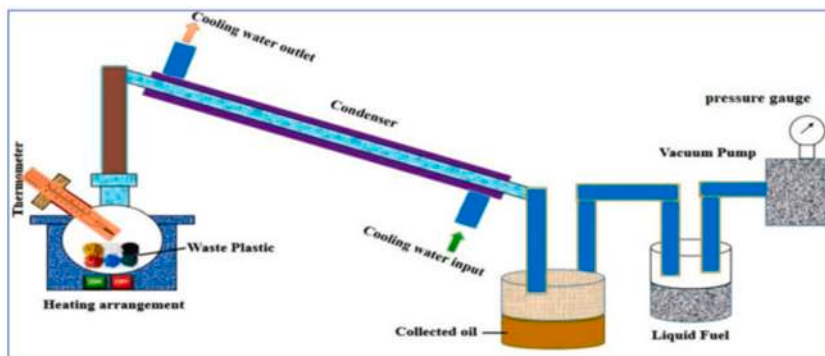

Fig. 2. Pyrolysis set-up [31].

Table 1
Properties of diesel and WPO with blended mixtures.

Parameters	Diesel	WPO	WPO10	WPO20	WPO30
Calorific Value (kJ/kg)	42,500	37,120	41,962	37,712	40,886
Sp. gravity	0.830	0.875	0.835	0.839	0.844
Kinematic viscosity (mm^2/sec)	3.05	5.5	3.3	3.54	3.79
Flash point (°C)	56	42	54.6	53.2	51.8
Cetane number	43	51	43.8	44.6	45.4

Table 2
Economic analysis of waste plastic oil (WPO).

Parameter	Cost (Rs.)	Remarks
Cost of plastic collection	Rs.5000 per ton	Waste plastic collected from the local and private organization
Waste plastic pyrolysis	Rs.18000 per ton	It includes electricity, fuel, labour and maintenance
Yield of waste plastic oil	60 % by weight	600 L of WPO per ton
Total production cost of WPO	Rs. 50 per Liter	Include all the costs like collection, processing and production.

2.2. Nanoparticles

In recent years, various nano additives such as cerium oxide, manganese oxide, alumina oxide, copper oxide, titanium oxide, zirconium oxide, zinc oxide, magnesium oxide, ferric oxide, and others have been utilized as fuel catalysts to improve combustion efficiency. Extensive research on these additives has been documented in numerous review papers. Experimental results from previous studies indicate a notable improvement in brake thermal efficiency along with a reduction in harmful engine emissions. In this study, a waste plastic oil biodiesel blend (WPO 20) is enhanced with alumina oxide as a nano fuel catalyst to evaluate its engine performance compared to standard fuel.

Alumina nanoparticles acts as a combustion catalysts due to its high thermal conductivity and surface area, promoting efficient heat transfer and improved oxidation during combustion. This results in better energy release and reduced formation of harmful emissions, such as carbon monoxide and particulate matter. Additionally, Al_2O_3 nanoparticles contribute to stabilizing the fuel mixture, enhancing atomization, and improving the overall combustion process, making the WPO20 blend more efficient and environmentally friendly for diesel engine applications Jin et al. [32].

The properties of alumina nanoparticles are presented in below Table 3.

A novel method for enhancing the characteristics of biodiesel involves the dispersion of metallic nanoparticles. By utilizing a Magnetic stirrer and an Ultrasonicator (Model: larsbo5200, 120W, 40 kHz), aluminium oxide (Al_2O_3) nanoparticles along with span 20 are combined with WPO20 blend to get a uniform nano additive blend. These are conducted at the research facilities of Nano wings private limited. The nano additives, with accurately measured mass fractions of 50 ppm and 100 ppm, were evenly distributed in the WPO20 blend using an Ultrasonicator operating at a frequency of 40 kHz and 120 W for 30 min. This process ensured the creation of consistent nanoparticles within the waste plastic oil.

2.3. Response surface methodology

Response Surface Methodology (RSM) is a set of statistical and mathematical approaches aimed at modeling and analyzing issues in which numerous factors affect a response of interest. This approach is particularly helpful for the optimization of processes aiming at the identification of the ideal circumstances for desired results. Historically, RMS became a potent instrument for industrial research in the 1950s mostly due to the pioneering efforts of George Box and others. Box's creative ideas prepared the way for the methodical

Table 3
Properties of Al_2O_3 nanoparticles.

Nano additive	Al_2O_3
Physical appearance	
Phase	alpha (α) phase
Crystallite size	20 nm
BET surface area	20 m^2/g
Shape	Spherical
Purity	99.9 %
Form	Powder
APS	50–200 nm

investigation of multi-dimensional response surfaces, therefore allowing researchers and engineers to efficiently probe difficult interactions among variables. RSM is used in historical data context to leverage already acquired data to increase the effectiveness and efficiency of experimental designs. This method helps one to find important elements and interactions affecting the answer variable. Analyzing past data helps researchers create prediction models that reflect the fundamental trends and connections in the data, therefore offering insightful information that can direct the next studies or process improvements.

Usually starting with the gathering of historical data on the factors of interest and their respective reactions, the process starts Data of this kind can come from observational research, historical experiments, or manufacturing runs. After the data is collected, statistical methods including regression analysis are used to fit the response variable to the independent factors. Usually approximating the response surface, the produced model forms a Polyn equation. Using historical data in RMS is one of the main benefits in terms of time and experimental expense savings. Using already available data helps researchers avoid pointless experiments and concentrate on improving the models depending on past observations. Moreover, historical data can offer a larger background that enables researchers to spot trends and patterns possibly not clear in small-scale studies. This can improve knowledge of varying interactions and result in more accurate responses under diverse situations predictions. Furthermore, RSM using past data helps to perform sensitivity analysis, therefore enabling researchers to evaluate how variations in input factors affect output response. This study helps to identify important thresholds and ideal operating conditions, therefore supporting decision-making procedures. Simulating several scenarios depending on historical data improves the validity of the results and finally helps to develop better optimization plans.

Finally, RSM's historical data method marks a major progress in experimental design and process improvement. Integration of historical data into the modeling process helps researchers create more accurate and dependable predictive models, simplify experimental efforts, and thereby increase process efficiency. This approach not only clarifies difficult systems but also provides a useful instrument for promoting creativity and ongoing development in many sectors [33].

2.4. Machine learning

Machine learning (ML) was used to develop predictive models for optimizing diesel engine performance with waste plastic oil blended with 1-butanol and alumina oxide nanoparticles. Trained on experimental data, ML accurately predicted key parameters like efficiency, fuel consumption, and emissions, enabling efficient optimization for improved performance and sustainability.

2.5. Random Forest

An ensemble learning method called Random Forest (RF) creates several decision trees and aggregates them to generate a more accurate and steady prediction. RF is fundamentally based on the idea of bagging, in which a subset of training data is randomly selected such that every tree may learn from many variants of the dataset. By averaging out the predictions of several trees to obtain a more generalized model, this approach lowers the risk of overfitting—a major problem experienced by individual decision trees. Every decision tree in the forest generates a forecast for every data point utilizing a sequence of binary splits depending on feature values. RF power comes from its capacity to efficiently manage both classification and regression problems. To guarantee diversity in the trees, it chooses at random a subset of features for splitting at every node during training. This variety adds to greater robustness and accuracy. Random Forest uses a majority vote in classification tasks or averages the outputs in regression tasks to make predictions, therefore lowering variance and improving performance [34].

RF's capacity to gauge feature relevance is another clear benefit. Examining the degree of each feature's contribution to the model's accuracy helps one to understand which variables most affect the predictions. In fields where knowledge of feature correlations is vital, this quality is especially helpful. Furthermore, Random Forest is rather simple to tweak; factors like the number of trees and maximum depth allow for variation in model complexity.

2.5.1. Gradient Boosting regression

Gradient Boosting Regression (GBR) is a powerful ML technique that builds predictive models in a stage-wise manner, combining the predictions of multiple weak learners to create a robust overall model. This method is based on the boosting idea, in which the next model is taught to fix mistakes produced by its previous. Gradient Boosting in the context of regression emphasizes reducing the residual errors of the past models, so iteratively improving predictions. Fundamentally, Gradient Boosting uses decision trees as the basic learners; usually utilizing shallow trees that capture patterns without overfitting, the approach starts with an initial prediction—usually a straightforward mean value—then adds later trees to the ensemble based on the gradients of the loss function. Gradient Boosting learns from its errors and progressively increases accuracy by matching a new tree to the residual mistakes of the current model. A key factor influencing the weight assigned to every new tree is the learning rate, hence balancing the convergence speed and stability of the model.

GBR's adaptability in managing many kinds of data and loss functions is among its main benefits. From financial forecasting to natural language processing, its versatility lets it be used in many different settings. Gradient Boosting is also fit for real-world datasets since it effectively handles missing values and categorical variables. To avoid overfitting, though, hyperparameter tuning—including tree depth and the number of boosting iterations—must be done. Furthermore, used to improve model generalization are regularizing methods. These properties taken together make GBR a preferred tool for creating very accurate predictive models among data scientists [35].

2.5.2. Decision tree

Based on a tree-like model of actions and their possible repercussions, Decision Tree Machine Learning is a generally applied method for both classification and regression problems. The method starts with a dataset having a target variable—which the model seeks to forecast—along with characteristics. Operating by recursively splitting the dataset according to the values of input attributes, decision trees generate branches leading to outcomes, or leaves, which reflect predictions. A fundamental element of decision tree building, the splitting criterion controls dataset division at every node. For regression, MSE is employed for model development. The aim is to choose splits that produce the most homogeneous groups thereby raising the predicted accuracy. The tree develops until it reaches a designated depth or until more splits have no appreciable effect on prediction quality. One of the main benefits of decision trees is their interpretability; the resultant model is accessible even to non-experts since it can be simply seen and understood. Following the journey from the root to the leaves lets users follow the decision-making process. However, as decision trees may collect noise in the training data rather than generalizable patterns, they are prone to overfitting especially when left to develop deep. Pruning and other methods can help to remove branches with minimal predictive value to solve this. Moreover, decision trees are quite flexible since they can manage numerical and categorical data without any preparation required. More sophisticated ensemble techniques, including Random Forest and Gradient Boosting, which seek to combine several decision trees to increase performance, also find roots in them. Due in great part to their simplicity and efficiency, decision tree algorithms are basic techniques in machine learning used extensively in many fields [36].

3. Experimental setup

The investigational unit is revealed in Fig. 3. The features of the engine are depicted in Table 4. The experimentation was performed on blended mixtures of WPOME and diesel. Performance, combustion and emission outcomes were analyzed in this study. The test rig is related with AVL burning study software. For emissions study AVL DI-Gas 444 gas analyzer and AVL 437 opacity calibration instrument are utilized. Experimental setup comprises of a diesel engine. The unit contain other panel which include fuel tank, air box, manometers, burette and temperature pointers. Oil intake is calibrated utilizing burette instrument. The air flow level is calculated by means of mass-air flow instrument. The dissipate gas is analyzed using the AVL gas analyzer.

4. Statistical results

Analysis of Variance (ANOVA) is a statistical tool widely used to evaluate the significance of multiple factors and their interactions on diesel engine characteristics. By partitioning the total variability in experimental data, ANOVA identifies the contributions of individual variables, such as fuel composition, engine load, or additives, to performance metrics like thermal efficiency, fuel consumption, and emissions. This analysis helps determine which factors significantly influence engine behaviour, ensuring a focused optimization process. ANOVA's ability to provide statistical validation makes it an essential tool for understanding and improving engine performance with alternative fuels. The results of ANOVA are presented in Table 5.

4.1. BTE model

Using the BTE model (Table 5), the analysis of variance (ANOVA) for the response surface quadratic model shows that the model is significant with a model F-value of 104.33, so reflecting an extremely low likelihood (0.01 %) of this outcome occurring owing to noise. The surface diagram and contour plot for BTE model is depicted in Fig. 4. With five degrees of freedom, the model's sum of squares comes out to be 407.94, yielding a mean square of 81.59. Significant model terms comprise A (p-value = 0.0001), B (p-value = 0.00291), and A^2 (p-value = 0.0001). Terms having a "Prob > F″ value higher than 0.1000, such AB and B^2, are not important and might be eliminated to increase the fit of the model. With a mean square of 0.78 and a residual sum of squares of 10.95, the fit is really good. While the adjusted R^2 is 0.9645, meaning the model is well-adjusted for the number of predictors, the R^2 value of 0.9739

Fig. 3. Experimental set-up [15].

Table 4
Engine specifications.

Engine category	Kirloskar
Power and speed	5.2 kW 1500 rpm
Bore(D)	87.5 mm
Stroke(L)	110 mm
Displacement-volume(V)	661.45cc
Compression-ratio (CR)	17.5:1
No. Of cylinders	01
Orifice diameter	20 mm
Type of cooling	Water cooled

indicates that the model explains around 97.39 % of the variance in the data. The model's dependability is supported by the expected R^2 (0.9544), which agrees rather well with the adjusted value. Strong signal-to-noise ratio indicated by the appropriate precision ratio of 26.563 indicates that the model is fit for negotiating the design space well beyond the intended value of 4.

4.2. BSFC model

The surface diagram and contour plot for BSFC model is depicted in Fig. 5. With an F-value of 74.21, the analysis of variance (ANOVA) for the response surface quadratic model in the BSFC (Brake Specific Fuel Consumption) model shows that the model is statistically significant—that is, with a very low likelihood—of this outcome occurring by random chance (Table 5). Spread across five degrees of freedom, the model sum of squares is 0.082, producing a mean square of 0.016. Significant are key elements including A (p-value 0.0001) and A2 (p-value 0.0001). Given their larger p-values, terms like B (p-value = 0.2852) and AB (p-value = 0.8237) are judged negligible, though. If not necessary for the model hierarchy, such words could be eliminated to improve the model still more. With a mean square error of 0.0002215 and a residual sum of squares of 0.0031, the model fit is really good. While the adjusted R^2 value of 0.9507 tests the robustness of the model when considering the number of predictors, the R^2 value of 0.9636 indicates that 96.36 % of the variability in the data is explained by the model. Reiterating the model's predictive power, the expected R^2 (0.9336) is near to the adjusted value. Exceeding the criterion of 4 with an appropriate precision ratio of 21.375, the model shows a strong signal-to-noise ratio, so a dependable instrument for efficiently investigating the design space.

4.3. HC emission model

With an F-value of 21.29, the ANOVA for the response surface quadratic model evaluating hydrocarbon (HC) emissions shows that the model is statistically significant and implies a very low likelihood (0.01 %) that the results happened by coincidence. The surface diagram and contour plot for HC model is depicted in Fig. 6. With a mean square of 533.67, the model's sum of squares—which spans five degrees of freedom—is 2668.35 Notable influence on HC emissions is shown by A (p-value = 0.0001) and A^2 (p-value = 0.0074). Conversely, factors like B (p-value = 0.2691) and AB (p-value = 0.9969) are not statistically significant and could be excluded to help to improve the model. With a standard deviation of 5.01, the residual sum of squares is 350.85, signifying somewhat modest data variability. Whereas the corrected R^2 of 0.8423 shows the model's performance following term adjustment, the R^2 value of 0.8838 indicates the model accounts for 88.38 % of the variability in HC emissions. Good predictive accuracy is shown by the projected R^2 of 0.7913, which is rather in line with the adjusted R^2. Moreover, the strong signal-to-noise ratio of the model is confirmed by the suitable precision ratio of 12.101, considerably over the minimum necessary value of 4, so providing a trustworthy instrument for design space navigation.

4.4. CO emission model

The surface diagram and contour plot for HC model is depicted in Fig. 7. Having an F-value of 24.20, suggesting an extremely low probability (0.01 %), the ANOVA for the response surface quadratic model analyzing carbon monoxide (CO) emissions demonstrates that the model is statistically significant. Spaced over five degrees of freedom, the total sum of squares for the model is 0.010, yielding a mean square of 0.002095. A (p-value 0.0001) and A^2 (p-value 0.0001) are important variables affecting CO emissions. But terms like B (p-value = 0.9189) and AB (p-value = 0.8131) are not significant, so their absence might improve the model's efficiency. With a standard deviation of 0.009302 and a residual sum of squares of 0.001212, the data shows a modest degree of fluctuation. While the modified R^2 of 0.8593 strengthens the validity of the model, an R^2 value of 0.8963 shows that the model explains 89.63 % of the variability in CO emissions. Reflecting the predictive ability of the model, the projected R^2 of 0.8167 fits the adjusted value rather nicely. Furthermore, the strong signal-to-noise ratio of the model, significantly higher than the required value of 4, is confirmed by its suitable precision ratio of 12.317, which makes it a useful instrument for investigating the design space.

4.5. NOx emission model

In the case of NOx emission model, the F-value of 516.31 obtained through ANOVA of NOx emission data shows that the model is quite significant and indicates almost no likelihood (0.01 %) of the results being impacted by noise. The surface diagram and contour

Table 5

ANOVA analysis.

|	BTE		BSFC		CO		HC		NOx		Smoke	
	F-value	p-value	F-value	p-value	F-value	p-value	F-value	p-value	F-value	p-value	F-value	p-value
Model	104.33	<0.0001	74.21	<0.0001	21.29	<0.0001	24.20	<0.0001	516.31	<0.0001	199.74	<0.0001
L	367.27	<0.0001	218.64	<0.0001	75.46	<0.0001	64.09	<0.0001	1955.77	<0.0001	732.17	<0.0001
C	5.91	0.0291	1.23	0.2852	1.32	0.2691	0.01	0.9189	0.45	0.5123	0.01	0.9363
LC	0.79	0.3894	0.05	0.8237	0.00	0.9969	0.06	0.8131	0.00	0.9665	0.10	0.7579
L^2	71.55	<0.0001	90.46	<0.0001	9.78	0.0074	42.27	<0.0001	97.42	<0.0001	84.17	<0.0001
C^2	0.76	0.3992	0.26	0.6193	0.03	0.8725	0.13	0.7233	17.49	0.0009	1.61	0.2256
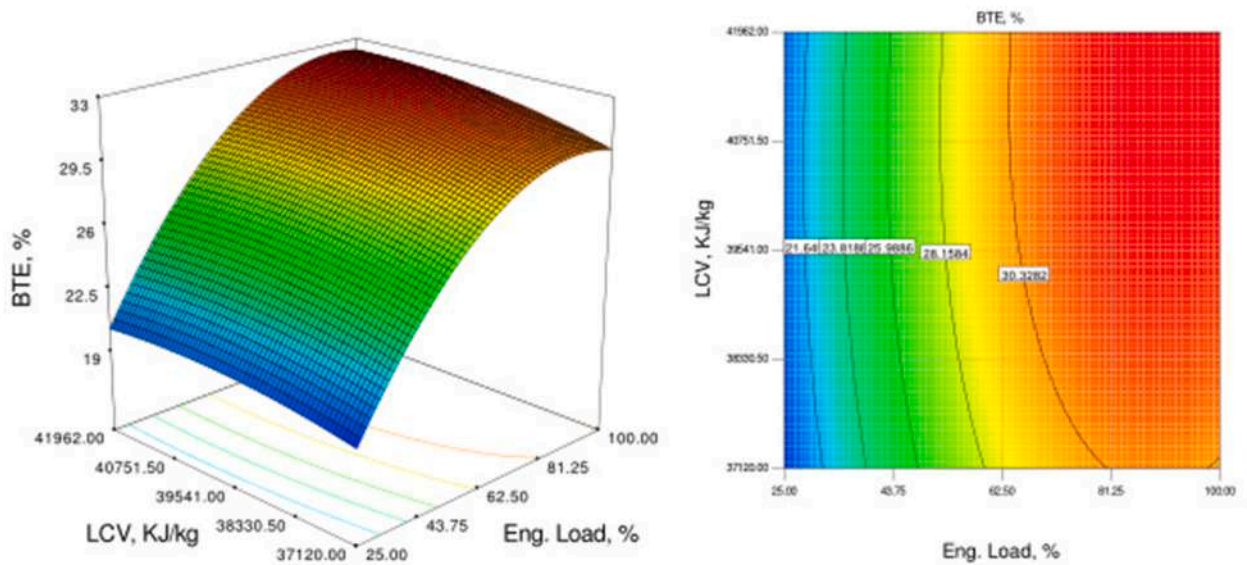
Fig. 4. BTE model LCV vs load (a) 3-d response surface (b) contour plots.
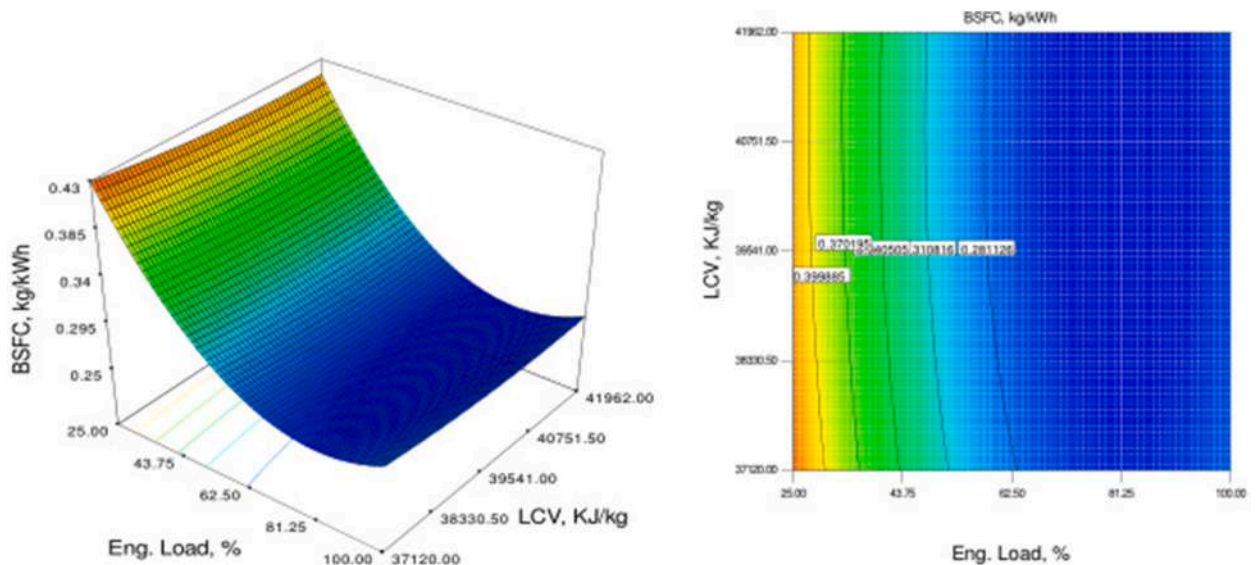
Fig. 5. BSFC model LCV vs load (a) 3-d response surface (b) contour plots.

plot for NOx model is depicted in Fig. 8. Computed from five degrees of freedom, the model's sum of squares is 5.327E+006, yielding a mean square of 1.065E+006. While B (p-value = 0.5123) and AB (p-value = 0.965) are not statistically significant, suggesting that they may be eliminated for model improvement, significant factors influencing NOx emissions include A (p-value = 0.0001), A2 (p-value = 0.0001), and B2 (p-value = 0.0009). With a standard deviation of 45.42 and a residual sum of squares of 28886.81, the data shows little variability. While the modified R^2 of 0.9927 further validates the model's resilience, its R^2 value of 0.9946 reveals that 99.46 % of the variance in NOx emissions is explained by the model. The model's predictive power is reinforced by the expected R^2 of 0.9899, which fits very precisely the adjusted value. Furthermore, the strong signal-to——noise ratio of the model, which far above the intended value of 4, is confirmed by the suitable precision ratio of 59.049, so providing a trustworthy instrument for negotiating the design space.

4.6. Smoke opacity model

With an F-value of 199.74, the ANOVA for the response surface quadratic model assessing smoke opacity reveals a very significant
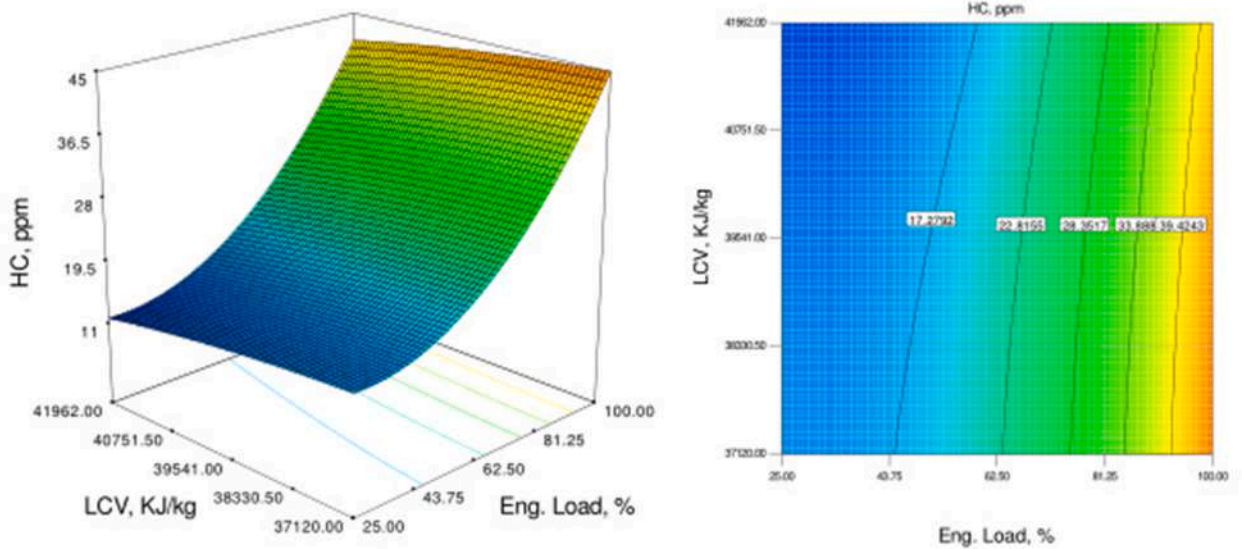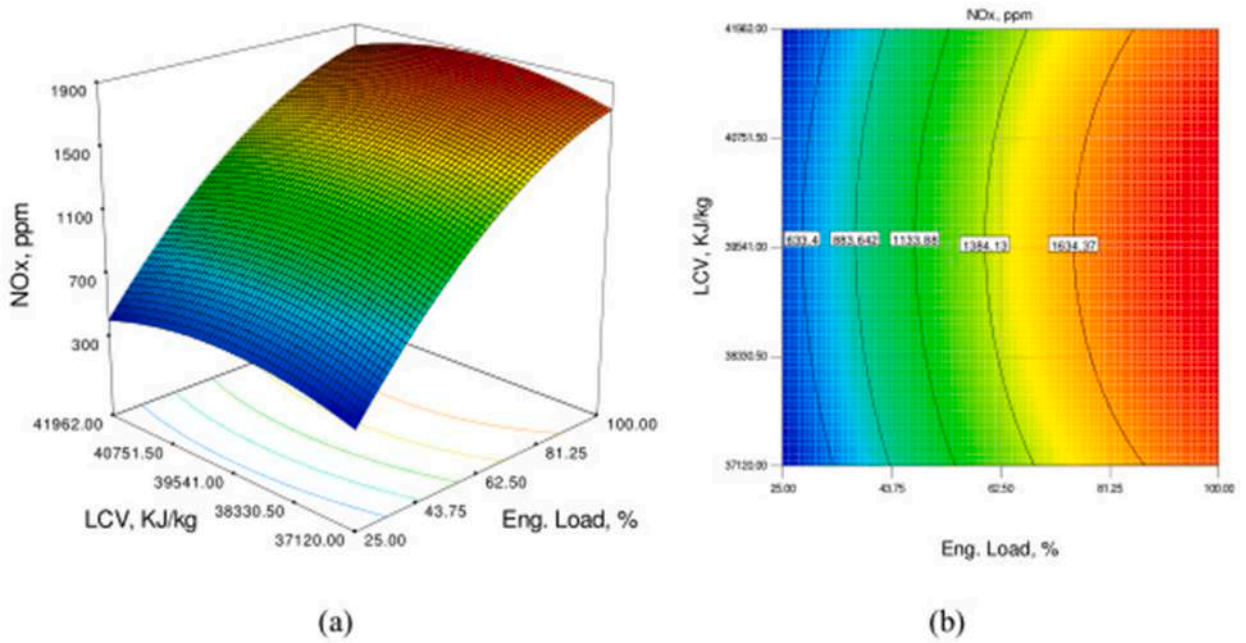
Fig. 6. HC model LCV vs load (a) 3-d response surface (b) contour plots.
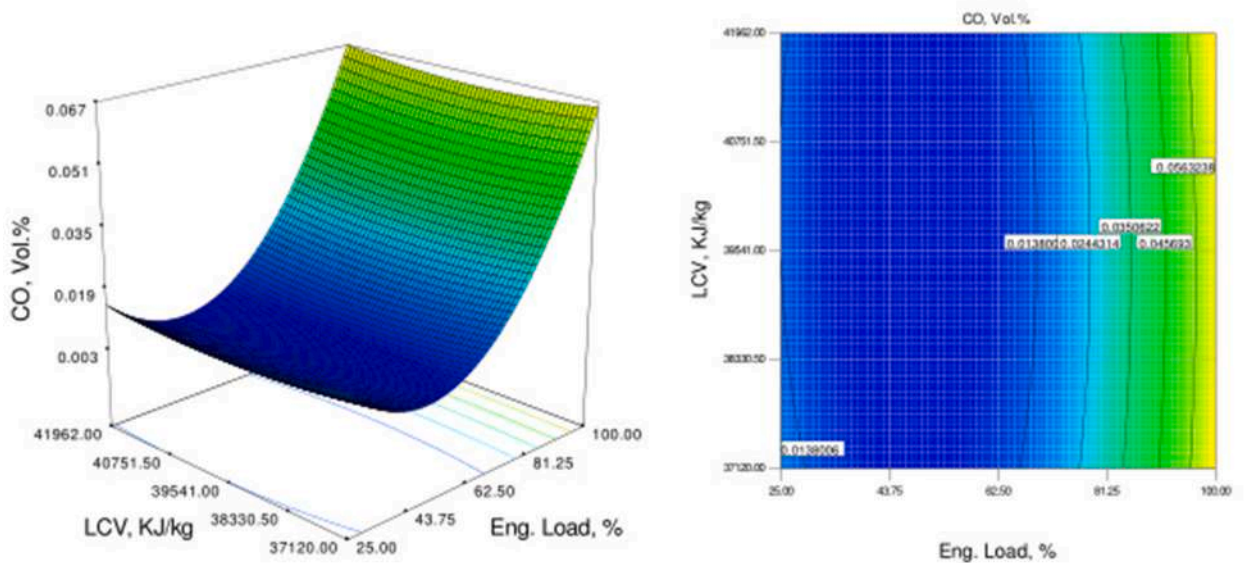
Fig. 7. CO model LCV vs load (a) 3-d response surface (b) contour plots.

model with a robust model fit with just a 0.01 % possibility that the results are attributable to noise. The surface diagram and contour plot for smoke opacity model is depicted in Fig. 9. With a mean square for the model being 2473.87, the total sum of squares is 12369.35. While terms B (p-value = 0.9363), AB (p-value = 0.7579), and B2 (p-value = 0.2256) are not statistically significant and might be eliminated to maximize the model, key factors influencing smoke opacity include factor A (p-value = 0.0001) and A2 (p-value = 0.7579). With a standard deviation of 3.52 and a residual sum of squares of 173.40, the residuals exhibit very little variability. While the modified R^2 of 0.9812 confirms the dependability of the model, the R^2 value of 0.9862 shows that the model explains 98.62 % of the variance in smoke opacity. Further confirming the model's predictive ability, the expected R^2 of 0.9776 fits quite precisely the modified R^2. Furthermore, the suitable precision ratio of 34.664 greatly surpasses the target value of 4, so verifying the strong signal-to-noise ratio of the model and enabling efficient use of it to traverse the design space.

4.7. Optimization

RSM uses desirability-based optimization to find ideal settings in multi response system. Models including BTE, BSFC, HC, CO, NOx,

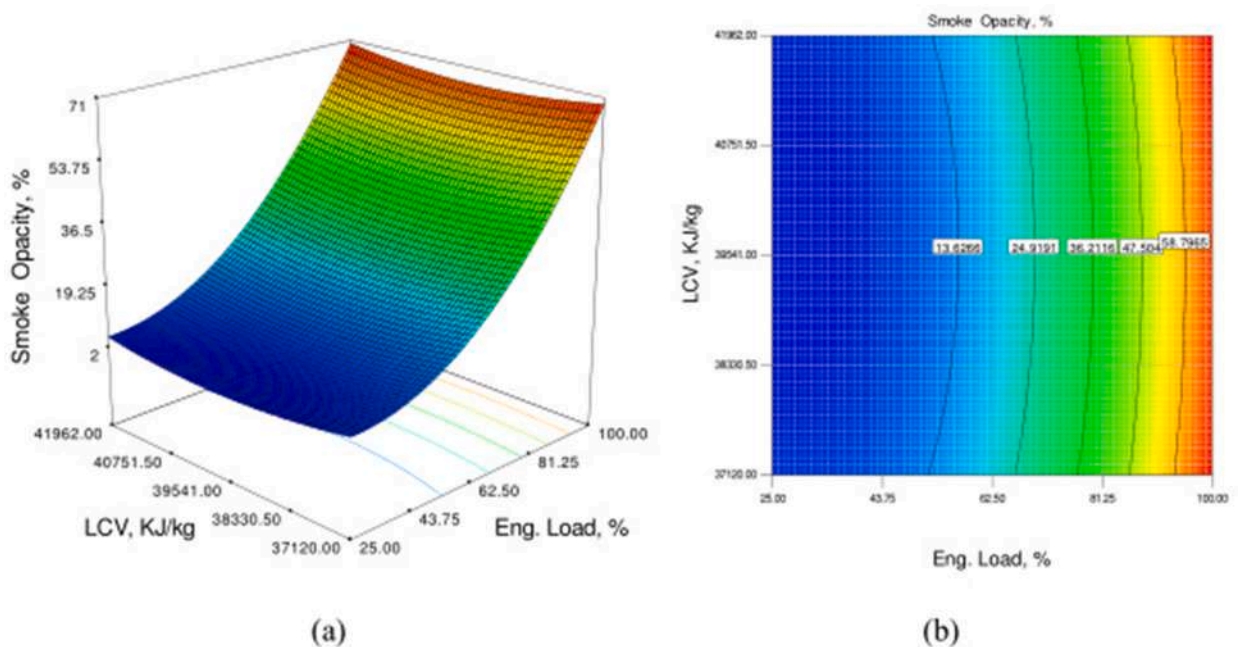**Fig. 8.** NOx model LCV vs load (a) 3-d response surface (b) contour plots.

Fig. 9. Smoke emission model LCV vs load (a) 3-d response surface (b) contour plots.

and Smoke Opacity were subjected in this work for optimization. Verified by ANOVA, the models displayed notable F-values and high R-squared values suggesting most of the response variability was effectively captured. A group optimization was done by balancing several criteria including pollutants and engine efficiency using desire functions. For every model, individual desirability values were computed, therefore aggregating several goals into a single composite desirability index. To attain the best overall performance, this method let one adjust the input variables—such as load and LCV values of blended fuel.

A desirability-based optimization method yielded the best outcomes for the engine performance criteria. The engine load fell between 25 and 100 at 64.56, ideal. The fuel's lower calorific value (LCV) was optimized near its maximum limit at 41961.98. Brake

specific fuel consumption (BSFC) was lowest at 0.2679 while brake thermal efficiency (BTE) was increased to 30.39. Emissions of carbon monoxide (CO) and hydrocarbons (HC) were much lowered to 19.39 and 0.012 respectively. Smoke opacity dropped to 23.14 while nitrogen oxides (NOx) were lowest at 1343.02. The desirability levels for individual as well as total desirability is shown in Fig. 10. With an overall desirability of 0.776, the optimization revealed a well-balanced solution over all the parameters and these are shown in Table 6.

5. Machine learning-based model development

Machine learning (ML) was employed to develop predictive models for optimizing diesel engine performance using waste plastic oil blended with 1-butanol and alumina oxide nanoparticles. Experimental data were used to train and validate the models, focusing on key engine parameters such as brake thermal efficiency, specific fuel consumption, and emissions. The ML models provided accurate predictions and insights, enabling efficient tuning of operating conditions for improved performance and reduced emissions, demonstrating the potential of ML in sustainable fuel applications.

5.1. Data pre-analysis based on correlation values

Using a correlation heat map and correlation matrix, data pre-analysis examined variable interactions. Whereas the correlation matrix gave numerical correlation values, the correlation heat map graphically showed the strength and direction of relationships. This method directed feature selection for the next analysis in the modelling phase and helped find important variables, and perhaps multicollinearity problems. The correlation heat map is depicted in Fig. 11a while correlation pair plots are illustrated in Fig. 11b.

The correlation matrix is listed in Table 7. The correlation matrix offers an entire picture of the connections among several factors influencing engine performance. Every item in the matrix shows, between -1 and 1, the correlation coefficient between two variables. A score of 1 indicates a perfect positive correlation—that is, the other variable increases too as one variable does. On the other hand, a value of -1 denotes a perfect negative correlation—that is, where a rise in one measure results in a fall in the other. For engine load and NOx emissions (0.97), for example, the matrix shows a high positive association; for brake thermal efficiency (BTE) and brake specific fuel consumption (BSFC), it displays a substantial negative correlation. This implies that while improved efficiency results in lower fuel consumption, more NOx usually results from higher engine loads. Moreover, HC emissions are favourably linked with CO (0.93) and HCU (0.95), meaning that CO and unburned hydrocarbons increase together as HC emissions grow. Maximizing engine performance and emissions depends on an awareness of these relationships since it enables one to choose which factors can be changed to get desired results in fuel economy and pollutant emissions. In thermal engineering, this matrix is a useful instrument for data analysis generally.

5.2. Engine performance and emission models

5.2.1. Brake thermal efficiency

The BTE prediction model was prepared using the data collected from lab-based testing results. In both training and testing sets, the performance measures of several models—including Random Forest (RF), Decision Tree, and Gradient Boosting Regression (GBR)—indicate differing degrees of efficacy (Table 6). The models are compared in Fig. 12(a–c). Reflecting great accuracy, the Random Forest model obtained a mean squared error (MSE) of 0.12 during training; its testing MSE was substantially higher at 1.63. At 0.9936 for the training set, the coefficient of determination, R^2, was good; nevertheless, it dropped to 0.9276 for the test set, indicating considerable over fitting. Though it exhibited a testing MSE of 1.60, leading to an R^2 value of 1.0000 in training and 0.9291 in testing, the Decision
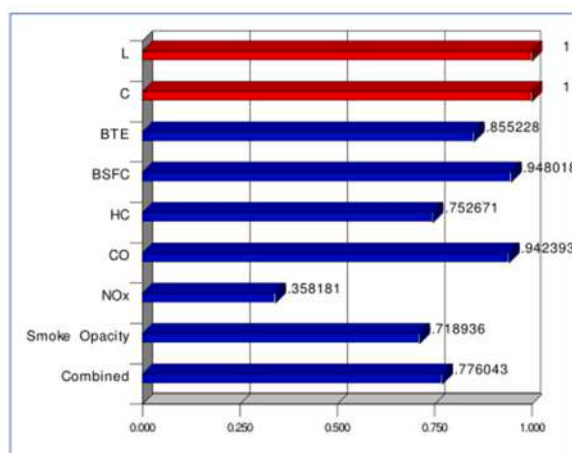

Fig. 10. Desirability levels.

Table 6
Optimized results.

Name	Goal	Lower value limit	Upper value limit	Optimized value
Load	within range	25	100	64.56
LCV	within range	37120	41962	41961.98
BTE	maximize	18.76	32.25	30.3877
BSFC	minimize	0.259	0.45	0.267877
HC	minimize	9	50	19.38586
CO	minimize	0.007	0.086	0.012012
NOx	minimize	418	1843	1343.024
Smoke Opacity	minimize	3.6	71.2	23.14293
Total desirability				0.776
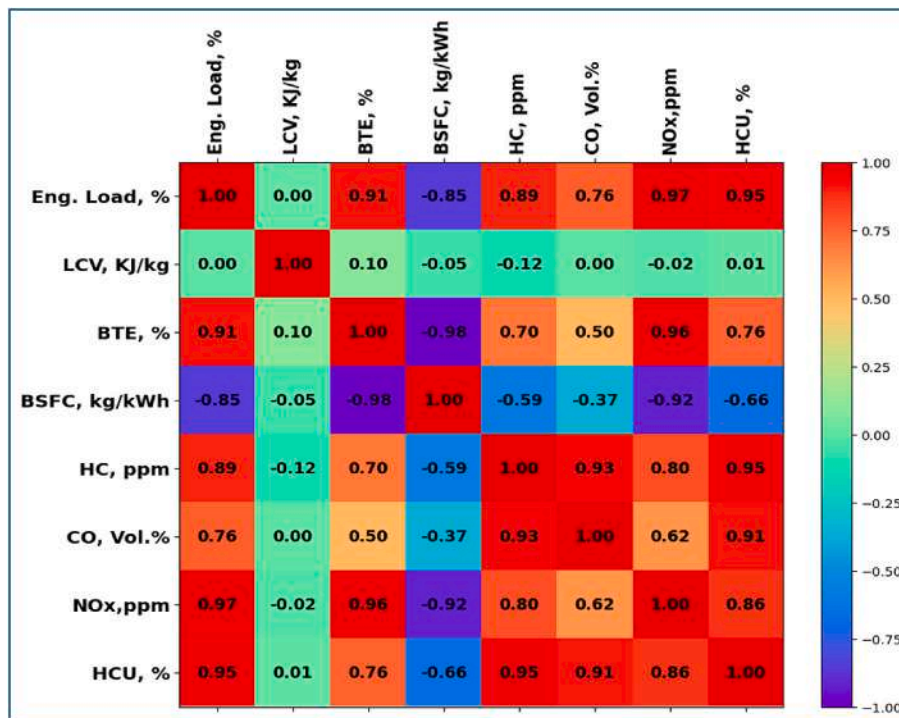
Fig. 11 (a). Heat map of correlation.

Tree model displayed an amazing training MSE of 0.00, suggesting a perfect match. With R^2 values of 0.9997 and 0.9180 for training and testing respectively, the GBR model reported a training MSE of 0.01 and a test MSE of 1.85. Furthermore, the Mean Absolute Percentage Error (MAPE) values for all models were rather low; RF showed 1.04 % for training and 5.23 % for testing; nevertheless, Decision Tree and GBR showed MAPE values of 0.00 % and 0.22 % respectively. These findings show generally the good performance of the models as well as the need to strike a balance between fit between training and testing sets. Given its almost perfect match to the training data, the Decision Tree model turned up as the best-performing method overall in this situation. ML prediction results are shown in Table 8.

5.2.2. Brake-specific fuel consumption

Data gathered from lab-based testing findings helped to create the BSFC prediction model. The performance evaluations of numerous models including RF, DT, and GBR show different degrees of efficacy in both training and testing sets, as listed in Table 8. Focusing on mean squared error (MSE), (R^2), and mean absolute percentage error (MAPE), three machine learning models—Random Forest (RF), Decision Tree (DT), and Gradient Boosting Regression (GBR)—can have their performance compared based on their training and testing metrics. With a train MSE of 0 and (R^2) of 1.0000 the Decision Tree attained flawless training outcomes, therefore suggesting a perfect fit to the training data. Its performance was greatly reduced during testing, therefore its test MSE of 0.000335 and test (R^2) of 0.9230 points to overfitting. With a higher test MAPE of 4.48, however, with a train MSE of 5.00E-05 and test MSE of 0.000167, RF displayed more balanced outcomes while keeping an amazing train (R^2) of 0.9875 and test (R^2) of 0.9616, thereby performing strongly in both training and testing stages. It likewise got modest MAPE values—1.84 for training and 3.82 for testing. With 0 MSE and an almost perfect (R^2) of 0.9995, GBR produced outstanding training performance. Its test MSE of 0.000182 and test
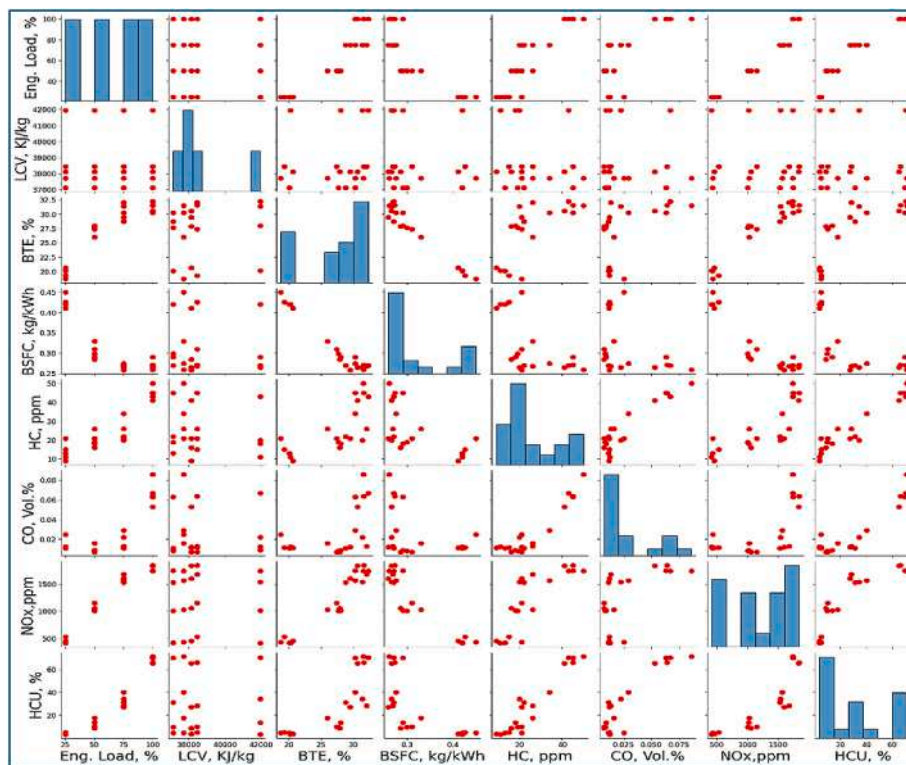
Fig. 11 (b). Correlation pair plot.

Table 7
Matrix of correlation.

	Eng. Load, (%)	LCV, KJ/kg	BTE, (%)	BSFC, kg/kWh	HC, ppm	CO, vol%	NOx, ppm	HCU, (%)
Eng. Load, %	1	0	0.91	−0.85	0.89	0.76	0.97	0.95
LCV, KJ/kg	0	1	0.1	−0.05	−0.12	0	−0.02	0.01
BTE, %	0.91	0.1	1	−0.98	0.7	0.5	0.96	0.76
BSFC, kg/kWh	−0.85	−0.05	−0.98	1	−0.59	−0.37	−0.92	−0.66
HC, ppm	0.89	−0.12	0.7	−0.59	1	0.93	0.8	0.95
CO, vol%	0.76	0	0.5	−0.37	0.93	1	0.62	0.91
NOx, ppm	0.97	−0.02	0.96	−0.92	0.8	0.62	1	0.86
HCU, %	0.95	0.01	0.76	−0.66	0.95	0.91	0.86	1
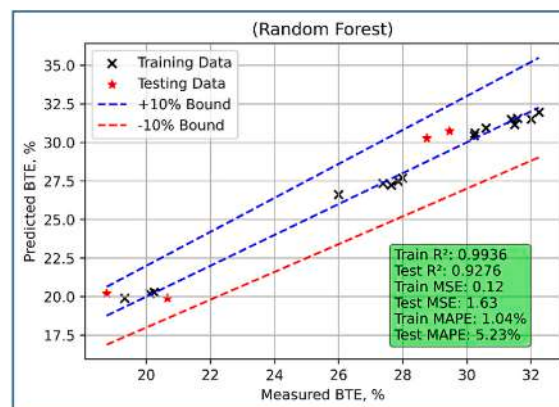
Fig. 12. BTE model comparison using (a) RF.
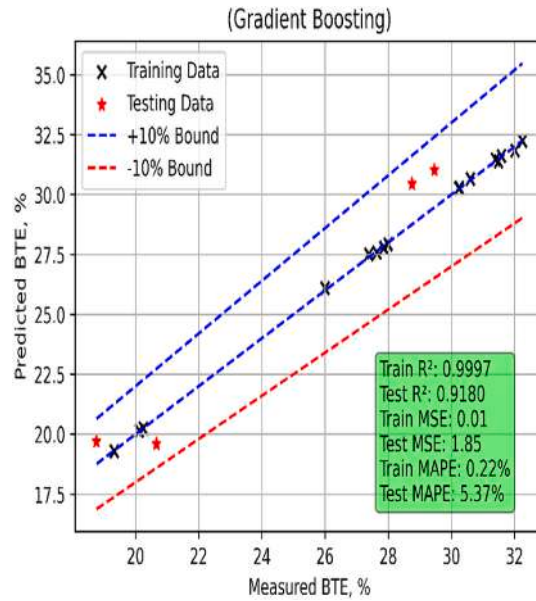
Fig. 12. BTE model comparison using (b) GBR.
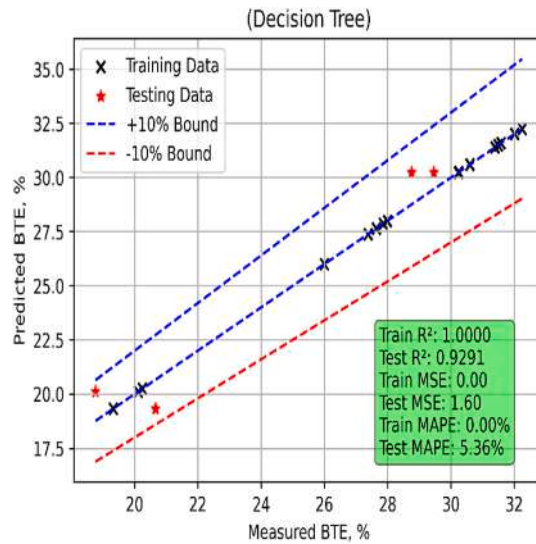
Fig. 12. BTE model comparison using (c) DT.

(R^2) of 0.9581 showed just a minor decline in performance during testing. The models are compared in Fig. 13(a–c). With a test MAPE of 3.80, GBR also achieved the best accuracy in forecasting unprocessed data. With great accuracy and low error rates in both stages, Random Forest offered the most balanced performance overall across training and testing, therefore indicating it is the best model among the three.

5.2.3. HC emission model

In the case of the HC emission model again, using their respective measures, the performance comparison of three models Random Forest (RF), Decision Tree (DT), and Gradient Boosting Regression (GBR) for estimating HC emissions is listed in Table 8. With an MSE of 0.00 and a (R^2) of 1 the Decision Tree model demonstrated flawless accuracy in training. With a high test MAPE of 23.63, its test MSE of 18.75 and test (R^2) of 0.8917 indicate overfitting, nevertheless, since it performs noticeably worse on the test data. The models are compared in Fig. 14(a–c). Conversely, the RF model fared well balancing training and testing. Its test MSE was 10.77 and its train MSE was 4.14; its train (R^2) was 0.9710 and its test (R^2) was 0.9 Dharma. Although it still shows space for development, its test MAPE of 19.20 is modest relative to DT. The GBR model offered generally the most accurate forecasts. It obtained a test (R^2) of 0.9903 and a

Table 8
ML prediction results.

Model	MSE	MSE	R^2	R^2	MAPE, %	MAPE, %
Training/test	Training	Test	Training	Test	Training	Test
RF	0.12	1.63	0.9936	0.9276	1.04	5.23
Decision Tree	0.00	1.60	1.0000	0.9291	0.00	5.36
GBR	0.01	1.85	0.9997	0.9180	0.22	5.37
RF	5.00E-05	0.000167	0.9875	0.9616	1.84	3.82
DT	0.00	0.000335	1.0000	0.9230	0.00	4.48
GBR	0.00	0.000182	0.9995	0.9581	0.36	3.80
RF	4.14	10.77	0.9710	0.9378	8.54	19.20
DT	0.00	18.75	1.0000	0.8917	0.00	23.63
GBR	0.12	1.69	0.9992	0.9903	0.82	7.26
RF	0.00	0.00	0.98	0.82	10.96	45.52
DT	0.00	0.00	1.00	0.91	0.00	14.56
GBR	0.00	0.00	1.00	0.94	1.63	22.60
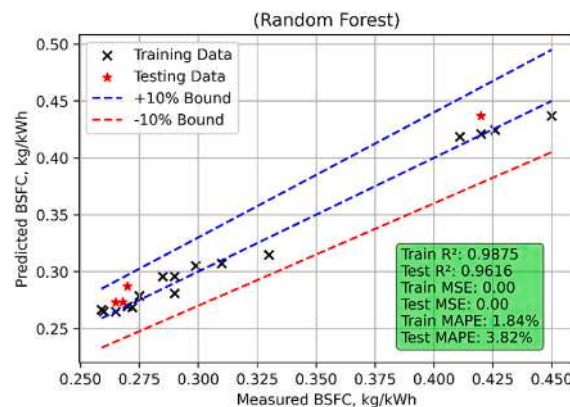
Fig. 13. BSFC model comparison using (a) RF.
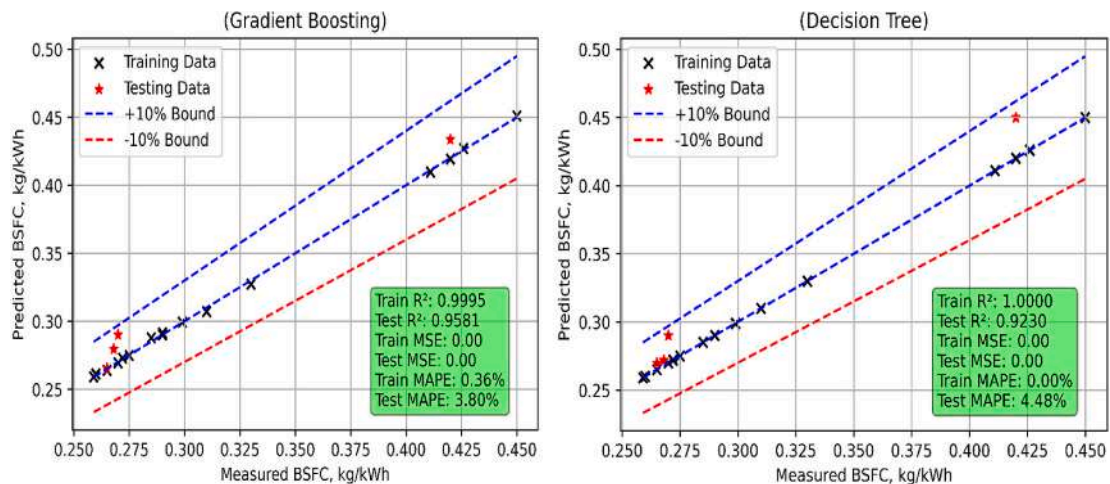
Fig. 13. BSFC model comparison using (b) GBR and (c) DT.

nearly flawless train (R^2). Among the three models, its test MSE of 1.69 and test MAPE of 7.26 were also much lower than those of the other models, so it was the most accurate and dependable for HC emission prediction. GBR therefore shows the lowest mistakes and best test accuracy among the models for HC emissions (Fig. 14).

5.2.4. CO emission model

In the case of the CO emission prediction model, with both the training and testing MSE being zero, showing no error in those
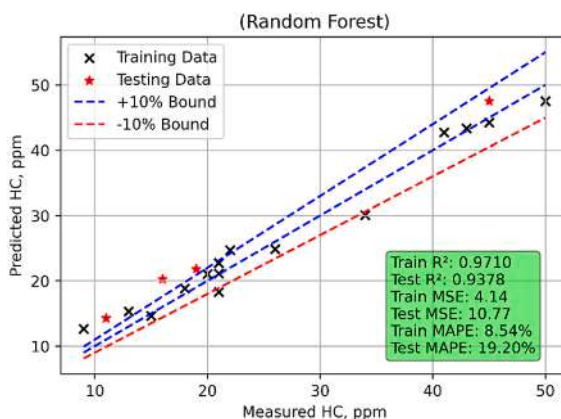
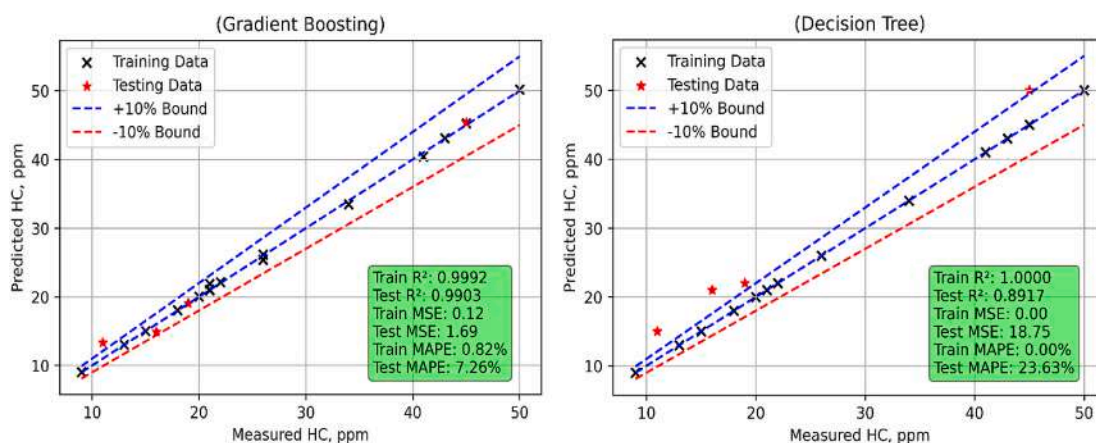**Fig. 14.** HC emission model comparison using (a) RF.

Fig. 14. HC emission model comparison using z(b) GBR (c) DT.

datasets, the RF model demonstrated outstanding training performance. The statistical results of model evaluation are listed in Table 8. The comparative performance of the model is shown in Fig. 15(a–c). In the case of the RF model, its test R^2 value, 0.82, indicated a minor decline in prediction accuracy on the test data relative to the DT and GBR models, though. Furthermore, showing notable variations in test predictions was the model's rather high test mean absolute percentage error (MAPE), at 45.52 %. With an R^2 score of 1.00 for training and 0.91 for testing, the DT model dominated both the training and testing stages. For both datasets, its MSE was zero; thus, it obtained a low test MAPE of 14.56 %, which makes it rather dependable for CO emissions projections. With a test R-squared value of 0.94 and 0 % MSE for both training and testing, the Gradient Boosting Regression model likewise fared rather well. Its test MAPE, however, was 22.60 %, more than DT even if it was less than RF. Given its general accuracy and low error rates, the Decision
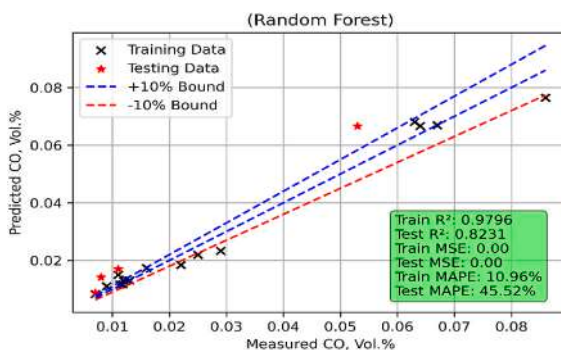

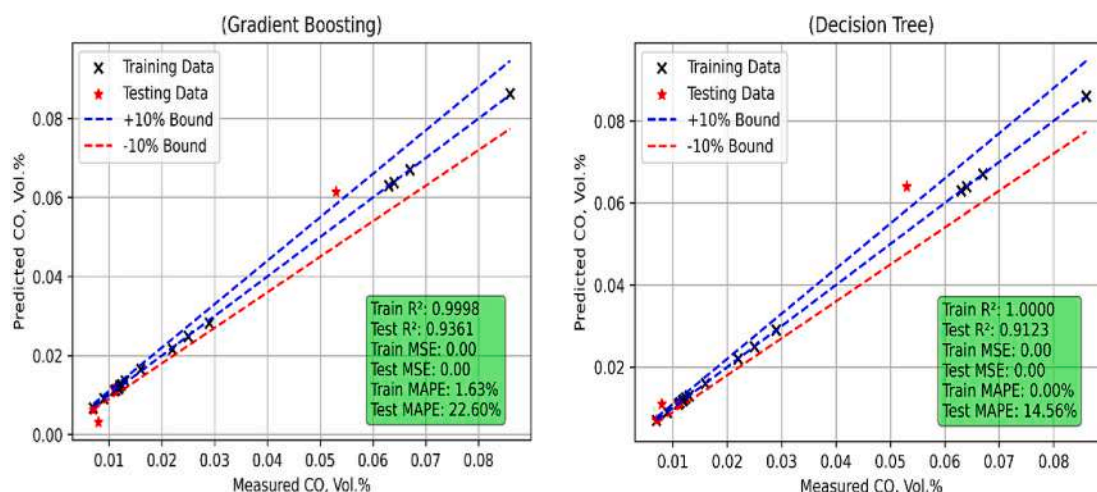**Fig. 15.** CO emission model comparison using (a) RF.

Fig. 15. CO emission model comparison using (b) GBR (c) DT.

Tree model thus stands out as the best for estimating CO emissions.

5.2.5. NOx emission model

Table 8 contains the statistical findings of the model evaluation. Fig. 16(a–c) displays the model's respective performance in comparison. With both the training and testing mean squared error (MSE) being zero, therefore showing no error in those datasets, the Random Forest model demonstrated outstanding training performance. Its test R-squared value, 0.82, indicated a minor decline in prediction accuracy on the test data relative to the Decision Tree and GBR models, though. Furthermore showing notable variations in test predictions was the model's rather high test mean absolute percentage error (MAPE), at 45.52 %. With an R-squared score of 1.00 for training and 0.91 for testing, the Decision Tree model dominated both the training and testing stages. For both datasets, its MSE was zero; thus, it obtained a low test MAPE of 14.56 %, which makes it rather dependable for CO emissions projections. With a test R-squared value of 0.94 and 0 % MSE for both training and testing, the Gradient Boosting Regression model likewise fared rather well. Its test MAPE, however, was 22.60 %, more than DT even if it was less than RF. Given its general accuracy and low error rates, the Decision Tree model thus stands out as the best for estimating CO emissions.

5.2.6. Smoke opacity model

In the case of smoke opacity also similar trends were observed. The statistical results of the model evaluation are presented in Table 8. Fig. 17a-c shows the corresponding performance of the model in respect. With a training mean squared error (MSE) of 2.23 and a testing MSE of 26.99 the RF model showed an excellent match on the training data but a modest degree of error when tested on the test data. Whereas the testing R^2 of 0.94 shows a high predicting ability on unknown data, its R-squared score of 1.00 for training reveals a perfect fit to the training data. However, the test mean absolute percentage error (MAPE) of 12.02 % shows some variations in its forecasts, especially concerning size. With an MSE of 0.00 and an R^2 of 1, the DT model proved to have a faultless training performance, thereby precisely reflecting the training data. Though having a rather bigger error than RF, its testing MSE of 20.33 and R-squared of 0.96 also show good performance. Although the test MAPE of 11.03 % shows that it performs rather well, its forecasts still show some errors. With a training MSE of 0.01 the GBR model fit the training data very exactly. Its MSE of 28.08, however, reveals a notable rise in inaccuracy when used on fresh data. While the testing R^2 dropped to 0.94, same to RF, the training R^2 was 1. Especially, the test MAPE of 44.07 % shows that GBR struggled with generalization despite its great training performance since its forecasts showed more substantial deviations than those of RF and DT. Overall, although all three models did well on the training set, the Random Forest model offered a balanced approach displaying competitive testing performance. Although the Decision Tree showed somewhat higher mistake in testing, it was outstanding in training accuracy. Although the Gradient Boosting model had great training accuracy, it suffered with generalisation and produced higher MAPE values in its forecasts.

6. Results and discussion on engine performance and emission features

6.1. Brake thermal efficiency

The brake thermal efficiency (BTE) of waste plastic oil-diesel blends, blend treated with 1-Butanol, Al₂O3 and diesel fuel is evaluated and observed the effect of 1-Butanol and Al₂O3. The disparity of BTE with load is shown in Fig. 18. The BTE of diesel is higher followed by WPO20 1-Butanol 5 %, WPO20 Al₂O3 100ppm, WPOME20, WPO20 1- Butanol 10 % and WPO20 Al₂O3 50ppm. As the load rises BTE of entire tested oils also rises. BTE of Diesel fuel is 33.58 %, WPO20 1-Butanol 5 % having 32.25 %, WPO20 Al₂O3 100ppm having 31.58 %, WPOME20 having 31.49 %, WPO20 1-Butanol 10 % having 31.3 % and WPO20 Al₂O3 50ppm having 30.6 %.
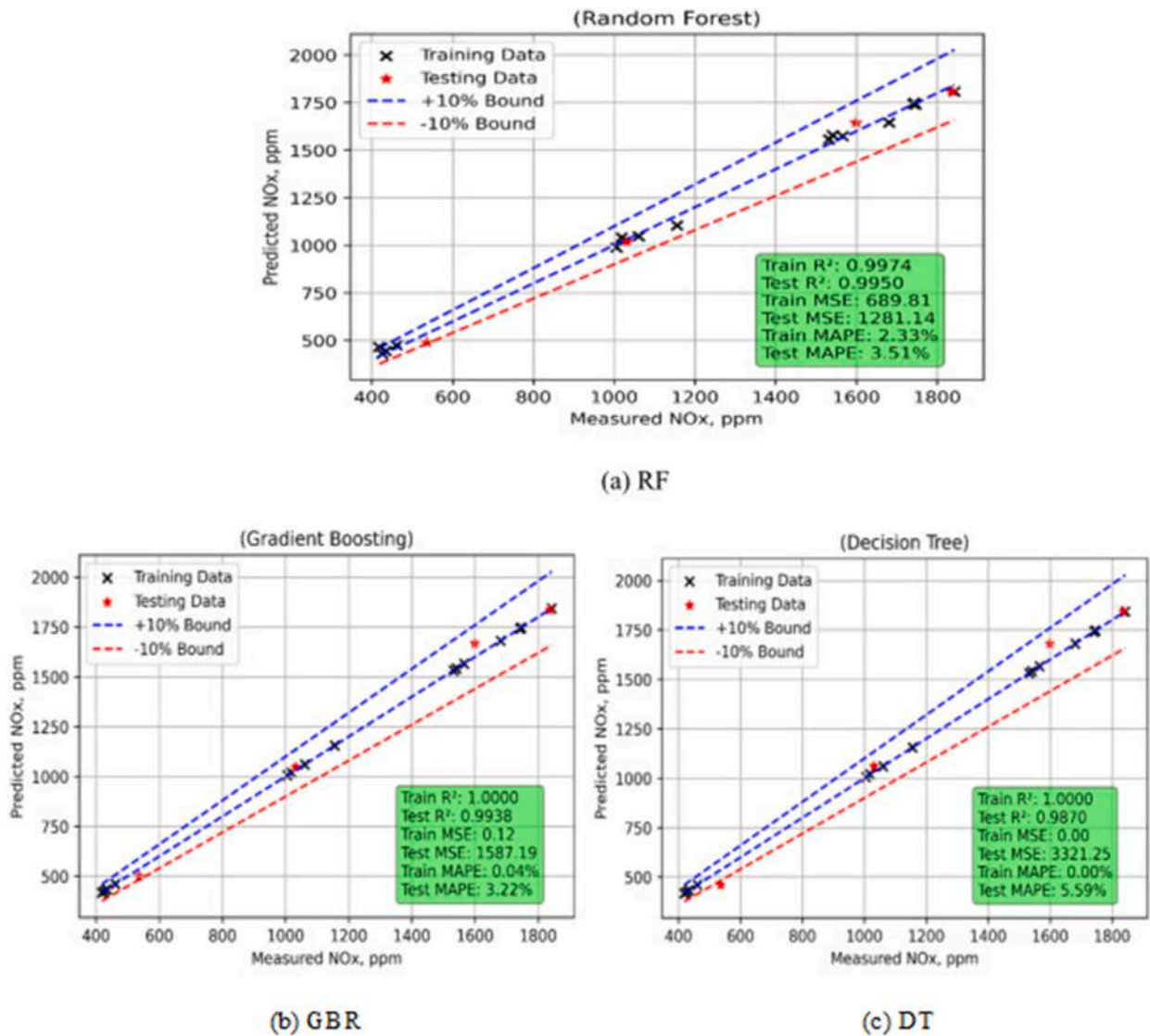
Fig. 16. NOx emission model comparison using (a) RF (b) GBR (c) DT.

Butanol has a higher cetane number, which indicates better ignition quality, and it also has a lower latent heat of vaporization. These properties lead to more efficient combustion, resulting in better thermal efficiency for Butanol added WPO20 blend compared to WPO 20 blend at all load conditions. The addition of butanol to diesel fuel offers several advantages that can contribute to increased brake thermal efficiency in diesel engines, including higher energy content, improved combustion characteristics, better miscibility, reduced emissions, and sustainability. Aluminum oxide nanoparticles can exhibit catalytic properties, facilitating the breakdown of hydro-carbon molecules and promoting more complete combustion. This catalytic effect can enhance combustion efficiency and contribute to higher thermal efficiency in diesel engines. The presence of nanoparticles in the fuel can improve heat transfer characteristics within the combustion chamber. This can lead to more complete combustion of the fuel-air mixture and better utilization of the energy released during combustion, thereby increasing thermal efficiency. The applications of fuel additives have shown increased engine performance reported by Ref. [37].

6.2. Brake specific fuel consumption

BSFC represents the amount of fuel consumed by an engine to produce a unit of power output. Specifically, BSFC is defined as the mass of fuel consumed per unit of power produced. BSFC is commonly used in the automotive industry and is an essential parameter for evaluating the efficiency of internal combustion engines, including diesel and gasoline engines. BSFC is commonly used in the automotive industry and is an essential parameter for evaluating the efficiency of internal combustion engines, including diesel and gasoline engines. From observation of experimental results, diesel brake specific fuel consumption (BSFC) is low on comparison with
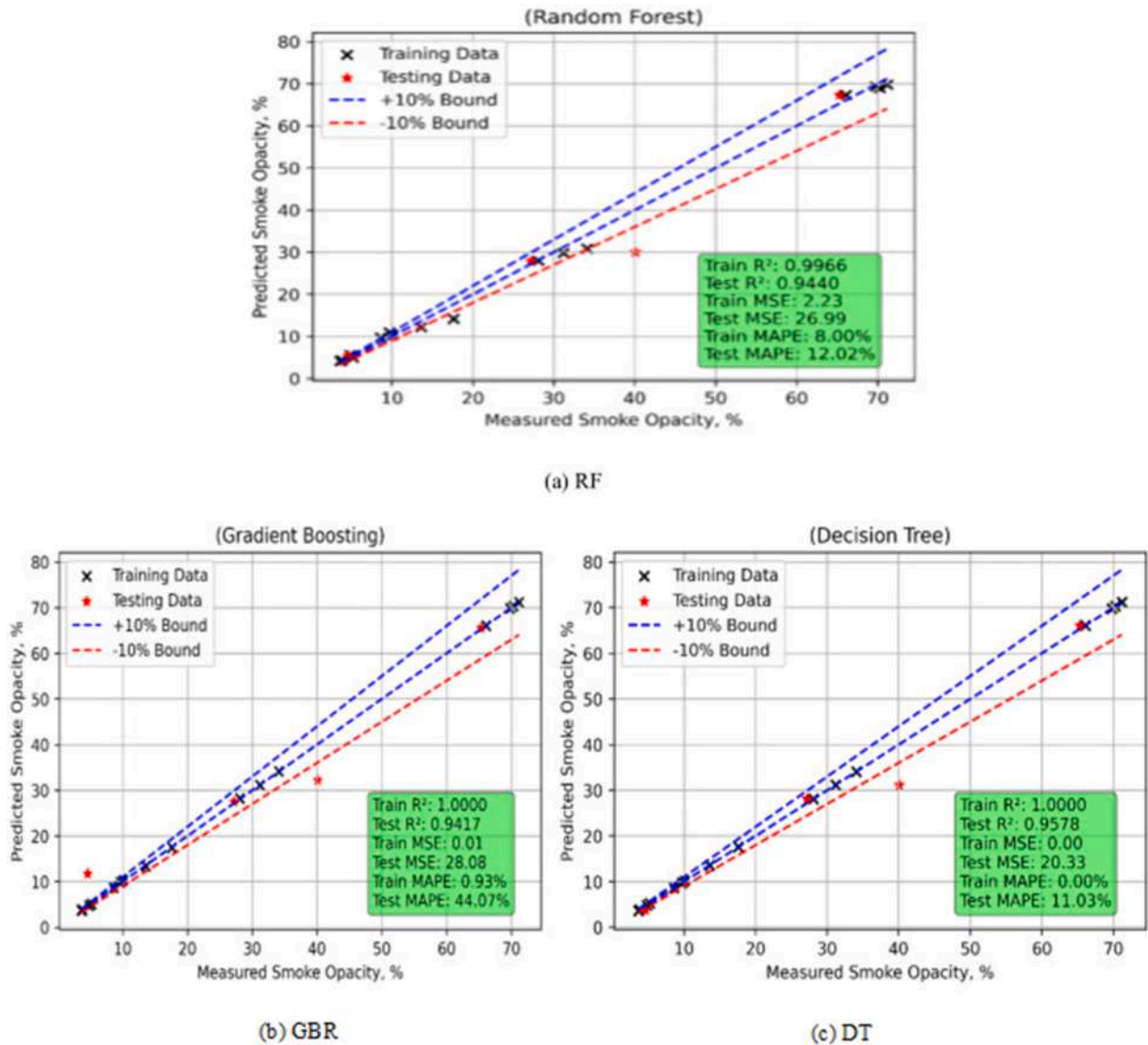
(a) RF

(b) GBR

(c) DT

Fig. 17. Smoke Opacity emission model comparison using (a) RF (b) GBR (c) DT.

other tested fuels. The disparity of BSFC with engine load is exposed in Fig. 19. BSFC of diesel is about 0.25kg/kWh followed by WPO20 1-Butanol 5 % having 0.27kg/kWh, WPO20 Al2O3 100ppm having 0.28kg/kWh, WPOME20 having 0.28kg/kWh, WPO20 Al2O3 50ppm having 0.29kg/kWh and WPO20 1-Butanol 10 % having 0.30kg/kWh at peak load. The main reason for the lower BSFC for the diesel fuel is due to higher calorific value when compared to the waste plastic oil as well as butanol added WPO20 blend. The addition of fuel additives like butanol and Al2O3 to the WPO20 is shown lower BSFC when compared to the WPO20 at full load. The present results were close confirmed with the results inferred by Ref. [38].

6.3. Exhaust gas temperature

EGT indicates the quality of combustion. Higher temperatures typically suggest complete combustion, whereas lower temperatures may indicate incomplete combustion, leading to higher emissions of unburned hydrocarbons and carbon monoxide. Exhaust Gas Temperature (EGT) refers to the temperature of the gases released during the combustion process. It is an important parameter in engine performance and monitoring because it reflects the efficiency of the combustion process and the load on the engine. The gas temperature at the time of exhaust stroke must be as high as possible for an engine which resembles the large power production, it is noticed that WPOME20, WPO20 1-Butanol 5 %, WPO20 1-Butanol 10 %, WPO20 Al2O3 50ppm and WPO20 Al2O3 100ppm has 385.25 °C,389.25 °C, 382.9 °C, 384 °C, 387.16 °C respectively. Compared to diesel, waste plastic oil blends have less exhaust gas temperature as presented in Fig. 20. Overall, it serves as a key indicator of engine health, combustion quality, and environmental
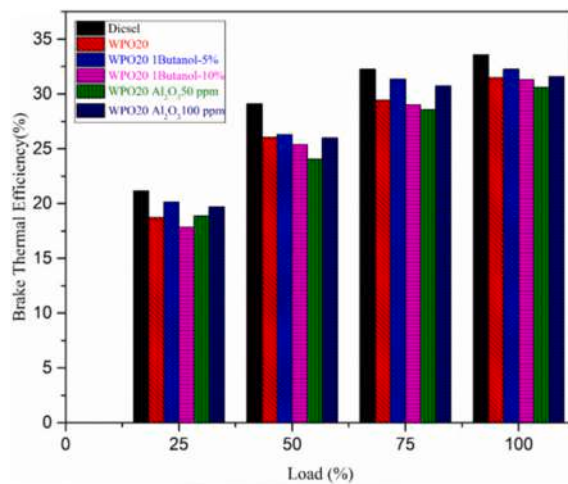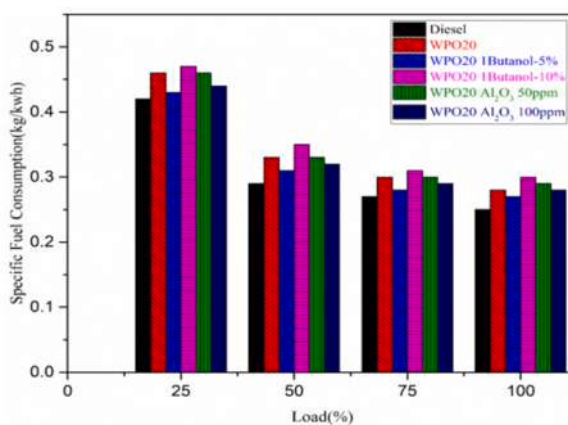
Fig. 18. BTE with engine load.

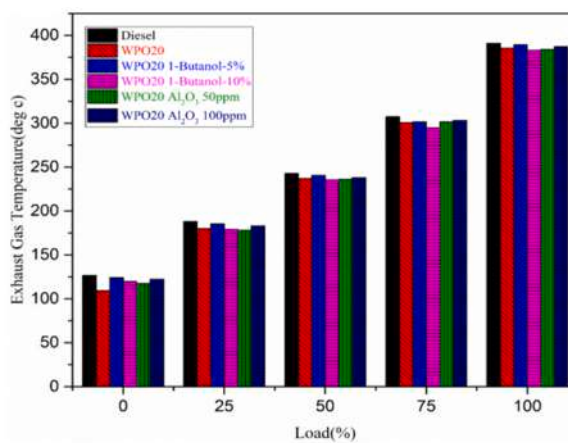**Fig. 19.** BSFC with engine load.

Fig. 20. EGT with engine load.

compliance.

6.4. Carbon monoxide

The variation of CO emissions with engine load for the examined fuels are delineated in Fig. 21. At full condition WPO20 Al_2O_3 100ppm having lower carbon monoxide emissions with 0.077 % followed by WPO20 1-Butanol 5 % with 0.08 %, WPO20 Al_2O_3 50ppm with 0.085 %, WPOME20 with 0.088 %, WPO20 1-Butanol 10 % with 0.089 % and diesel fuel with 0.09 %. based on the load rises, CO decreases. Butanol has a higher cetane number than conventional diesel fuel, which indicates better ignition quality. This can result in more stable combustion, reducing the likelihood of incomplete combustion events that produce CO. The presence of oxygen facilitates the oxidation of hydrocarbon molecules, leading to lower emissions of CO and other incomplete combustion byproducts. Overall, the use of butanol in biodiesel or diesel blends can contribute to the reduction of CO emissions by promoting more complete combustion, improving combustion stability, increasing oxygen content, lowering exhaust gas temperatures, and reducing engine deposits. Engine exhaust emissions were reduced with the applications of fuel additives reported by Sanjesh and Geetesh [39].

6.5. Hydrocarbons

Incomplete combustion can occur if the air-fuel mixture is not properly atomized or if combustion conditions are suboptimal. This can result in the release of unburned hydrocarbons into the exhaust. The properties of the fuel used can influence HC emissions. Factors such as fuel volatility, cetane number, and sulfur content can affect combustion efficiency and the likelihood of incomplete combustion, leading to higher HC emissions. From the experimental assessment, it is detected that the addition of 1-Butanol and Al2O3 causes decrease in hydrocarbons emissions (HC). The disparity of hydrocarbon discharges of 1- Butanol and Al2O3 fuel blended mixtures with engine load is shown in Fig. 22. WPO20 Al2O3 100ppm possesses low hydrocarbon emissions compared to all tested fuels with 45ppm at full load followed by WPO20 1-Butanol-5% with 48ppm, WPO20 1-Butanol-10 % with 50ppm, WPO20 Al2O3 50ppm with 53ppm, WPOME20 with 59ppm and Diesel fuel with 60ppm. As the load rises emissions of HC also rises. At higher loads, the fuel injected into the engine increases to meet the power demand. However, the air-fuel mixture may become richer, leading to zones with insufficient oxygen, resulting in incomplete combustion and higher HC emissions. At higher loads, the increased fuel injection rate may lead to poor atomization and uneven mixing of fuel and air, contributing to localized pockets of unburned fuel [40].

6.6. Nitrogen oxide

Nitrogen oxides (NOx), including nitrogen oxide (NO) and nitrogen dioxide (NO2), are produced in diesel engines due to the high temperatures and pressures in the combustion chamber, as well as the presence of nitrogen and oxygen in the air. Diesel engines operate at high compression ratios, leading to high temperatures in the combustion chamber during the combustion process. These high temperatures can cause nitrogen and oxygen from the air to react, forming NOx compounds. The excess air used in diesel engine combustion contributes to the formation of NOx. Oxygen present in the air combines with nitrogen from the combustion air to form NOx compounds. By the experimentation, addition of 1-Butanol and Al2O3 causes increase in NOx. The disparity of NO_X emissions with load of 1-Butanol and Al2O3 blended fuels is presented in Fig. 23. As the amount of 1-Butanol and Al2O3 increases NO_X increases. At zero load, WPO20 Al2O3 100ppm having 107ppm of NO_X followed by WPO20 1-Butanol-5% with 100ppm, WPO20 Al2O3 50ppm with 93ppm, WPOME20 with 80 ppm, WPO20 1-Butanol-10 % with 66ppm and Diesel Fuel with 62ppm. At full load condition, WPO20 Al2O3 100ppm having 2121ppm of oxides of nitrogen emissions followed by WPO20 1-Butanol-5% with 2092 ppm, WPO20 1-Butanol-10 % with 2087 ppm, WPO20 Al2O3 50ppm with 2059 ppm, WPOME20 with 2036 ppm, and Diesel Fuel with 1909 ppm. As the load rises NO_X also rises. The presence of oxygen improves the combustion process, leading to more complete combustion and
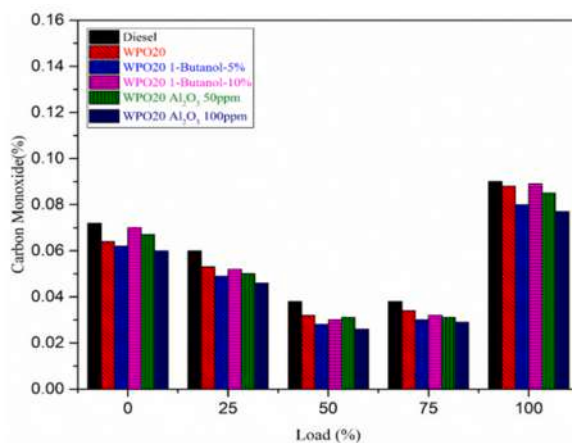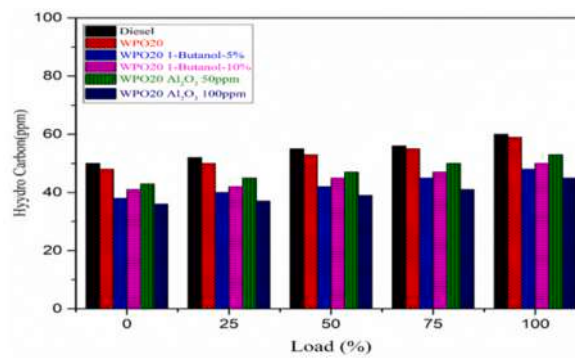

Fig. 21. CO with engine load.

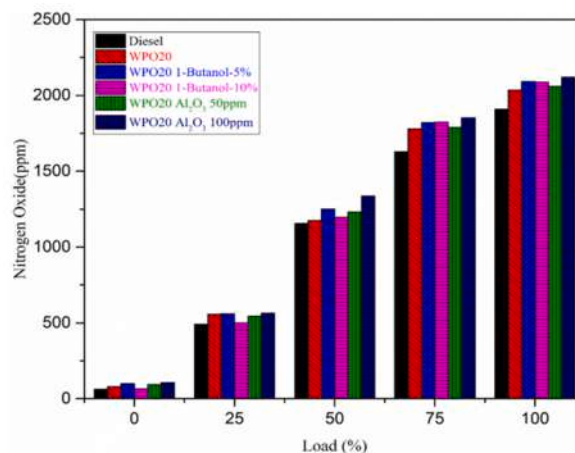**Fig. 22.** HO with engine load.

Fig. 23. NOx with engine load.

lower peak combustion temperatures. Since NOx formation is highly temperature-dependent (it forms at high temperatures), the reduction in peak temperature due to better combustion helps lower NOx emissions.

6.7. Smoke opacity

Diesel engines may experience incomplete combustion due to factors such as poor fuel atomization, inadequate mixing of fuel and
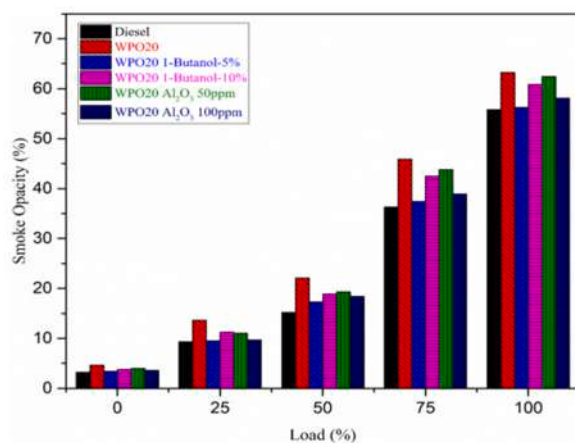

Fig. 24. Smoke with engine load.

air, insufficient combustion chamber temperatures, or incorrect fuel injection timing. When combustion is incomplete, unburned hydrocarbons and particulate matter are released into the exhaust as smoke. The quality of the diesel fuel used can affect smoke emissions. Low-quality or contaminated diesel fuel may contain impurities or higher levels of aromatics that contribute to incomplete combustion and increased smoke emissions. Excessive fuel injection or over fueling can lead to rich air-fuel mixtures, resulting in incomplete combustion and increased smoke emissions. This can occur due to factors such as incorrect fuel injection timing, worn injectors, or engine tuning issues. The addition of 1-Butanol and Al_2O_3 to WPOME20 opacity percentage increases but within acceptable limits. The disparity of opacity with load is exposed in Fig. 24. Opacity rises with rise in load on engine. At no load, WPOME20 having 4.6 % opacity of exhaust gases followed by WPOME20 Al2O3 50ppm with 4 %, WPO20 1-Butanol-10 % with 3.8 %, WPOME20 Al2O3 100ppm WITH 3.6 %, WPO20 1-Butanol-5% with 3.4 % and Diesel Fuel with 3.2 %. At full load condition, WPOME20 having 63.2 % opacity of exhaust gases followed by WPOME20 Al2O3 50ppm with 62.4 %, WPO20 1-Butanol-10 % with 60.9 %, WPOME20 Al2O3 100ppm WITH 58.1 %, WPO20 1-Butanol-5% with 56.3 % and Diesel Fuel with 55.8 %.1-butanol is an oxygenated fuel, meaning it contains oxygen within its chemical structure. This improves the fuel's combustion process by providing additional oxygen to the reaction. Better mixing and faster flame propagation reduce incomplete combustion, which is a primary cause of smoke emissions. Overall, the synergy between WPO20 and 1-butanol's properties enhances combustion efficiency and reduces soot formation, leading to lower smoke emissions compared to other blends. These results were in agreement with the reports presented by Ref. [41].

6.8. Cylinder pressure

Investigation of disparity of cylinder pressure (CP) with crank angle (CA) on engine fueled with diesel fuel, WPOME20, WPOME20 with addition of 1-Butanol and Al2O3 is plotted in Fig. 25. Fuel additives can influence the thermodynamics of combustion by altering the energy released during the process. Some additives enhance the energy density of the fuel, leading to higher combustion temperatures and pressures, while others may reduce energy losses through improved combustion efficiency. It is observed that the addition of 1-Butanol and Al2O3 causes increase in cylinder pressure. Lower cylinder pressures result in smaller ignition delay periods. At full load condition WPOME20 having lesser cylinder pressure compared to all tested fuels with 70.53 bar, WPO20 Al2O3 50ppm having cylinder pressure of 70.76 bar at 11 degrees of crank angle, diesel having 72.44 bar CP at 8 degrees of CA, WPO20 1-Butanol 10 % having cylinder pressure of 72.86 bar, WPO20 Al2O3 100ppm having cylinder pressure of 73.36 bar and WPO20 1-Butanol 5 % having higher cylinder pressure compared to all tested fuels with 74.94 bar at 9 degrees of CA.

6.9. Heat release rate

Experimental investigation on addition of 1-Butanol and Al_2O_3 to WPOME20 is observed and heat release rate is plotted as Fig. 26 along with CA at peak load condition. From the observation of Fig. 26, we can say that Additives can increase the heat release profile during combustion, affecting factors such as flame propagation speed and combustion stability. This can result in smoother and more controlled combustion, reducing the likelihood of engine knock or detonation. Fuel additives may influence the temperature distribution within the combustion chamber. By altering combustion kinetics, they can affect peak temperatures and temperature gradients, which in turn impact emission levels and engine performance. Due to lower CP the heat release rate (HRR) is reduced in WPO20 Al_2O_3 50ppm and WPOME20 blends. However, lower cylinder pressure triggers low ignition delay periods. At full load condition, WPO20 1-Butanol 5 % having greater HRR of 54.45 J/deg followed by WPO20 Al2O3 100ppm having 49 J/deg at −4 degrees of crank angle, Diesel Fuel with 45.24 J/deg of heat release rate WPO20 1- Butanol 5 % having 43.32 J/deg of heat release rate, WPO20 Al2O3 50ppm having 42.32 J/deg of heat release rate and WPOME20 having 41.32 J/deg of heat release rate at −2 degrees of crank angle.
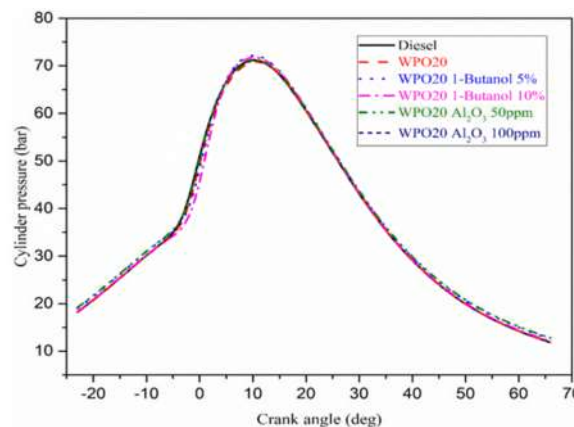

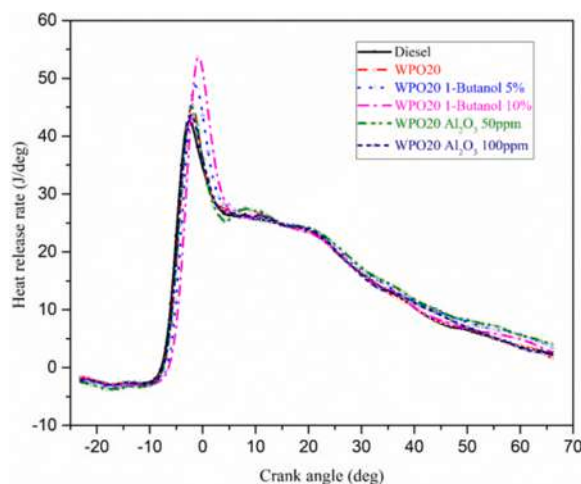**Fig. 25.** Cylinder pressure with crank angle.

Fig. 26. Disparity of Heat release rate with crank angle.

7. Conclusion

This current experimentally tested work analyzes that, engine's performance, and emission parameters fueled with diesel, waste plastic oil, 1-Butanol and Al_2O_3 blended bio-fuel trials were executed at 5 loads of 0 %–100 %. Fuel additive 1-Butanol and nano-particle Al_2O_3 is added to the waste plastic biodiesel at 5 %, 10 % and 50ppm, 100ppm on volume basis.

From this experimental investigation the following conclusions are made.

❖ The test results disclosed that WPOME20 has presented enhanced burning parameters like HRR and cylinder pressure related to the mixing of 1-Butanol and Al_2O_3 to the WPOME 20 blended mixture at peak load.
❖ Addition of 1-Butanol 5 % caused decrease in COs and HCs decreased by 9 % and 18.6 % correspondingly compared to WPOME20.
❖ Addition of nanoparticle Al_2O_3 100 ppm caused decrement in COs and HCs reduced by 12.5 % and 18.5 % correspondingly compared to WPOME20.
❖ Addition of 1-Butanol 5 % and Al_2O_3 100 ppm to WPOME20 resulted in slightly increase of oxides of nitrogen with acceptable limit.
❖ Optimized engine characteristics are found with the RSM-ML approach.

Ultimately, the novel 20 % waste plastic oil blend is suggested for diesel engine. Furthermore, the addition of 1-Butanol 5 % and Al_2O_3 100 ppm shown enhanced performance, combustion, and emission parameters.

CRediT authorship contribution statement

Jayashri N. Nair: Conceptualization. **T. Nagadurga:** Writing – original draft. **V. Dhana Raju:** Formal analysis. **Harish Venu:** Writing – original draft. **Sameer Algburi:** Project administration. **Sarfaraz Kamangar:** Supervision. **Amir Ibrahim Ali Arabi:** Supervision. **Abdul Razak:** Methodology. **Narasimha Marakala:** Investigation.

Declaration of competing interest

The authors declare that they have no known competing financial interests or personal relationships that could have appeared to influence the work reported in this paper.

Acknowledgement

Data availability

Data will be made available on request.

References

[1] K.H. Mudhee, et al., Assessing climate strategies of major energy corporations and examining projections in relation to Paris Agreement objectives within the framework of sustainable energy, Unconv. Resour. 5 (2025) 100127.

[2] A. Almack, "Different Types of Plastic," Knowledgebase.

[3] A.A. Abdullah, F.S. Attulla, O.K. Ahmed, S. Algburi, Effect of cooling method on the performance of PV/Trombe wall: experimental assessment, Therm. Sci. Eng. Prog. 30 (2022) 101273.

[4] Q. Hassan, S. Algburi, A.Z. Sameen, H.M. Salman, M. Jaszczur, A review of hybrid renewable energy systems: solar and wind-powered solutions: challenges, opportunities, and policy implications, Results Eng (2023) 101621.

[5] V. Modi, et al., Nanoparticle-enhanced biodiesel blends: a comprehensive review on improving engine performance and emissions, Mater. Sci. Energy Technol. (2024).

[6] V. Kumar, A.K. Choudhary, A comparative review on evaluation of performance, combustion, and emission characteristics of biodiesel blends enriched with hydrogen, additives and their combined effect, Therm. Sci. Eng. Prog. (2023) 102185.

[7] A. Prabu, Nanoparticles as additive in biodiesel on the working characteristics of a DI diesel engine, Ain Shams Eng. J. 9 (4) (2018) 2343–2349.

[8] L. Jeryrajkumar, G. Anbarasu, T. Elangovan, Effects on nano additives on performance and emission characteristics of calophyllim inophyllum biodiesel, Int. J. ChemTech Res. 9 (4) (2016) 210–219.

[9] H. Venu, P. Appavu, D. R V, Influence of Zr2O3 nano additives on particle size diameter (PSD), mass fraction burnt (MFB) and engine characteristics of Jatropha biodiesel fuelled DI diesel engine, Aust. J. Mech. Eng. 22 (2) (2024) 387–405.

[10] D. Swamy, et al., Effect of 1-butanol on the characteristics of diesel engine powered with novel tamarind biodiesel for the future sustainable energy source, Energy Sources, Part A Recover. Util. Environ. Eff. 45 (3) (2023) 6547–6565.

[11] A. Prabu, R.B. Anand, Emission control strategy by adding alumina and cerium oxide nano particle in biodiesel, J. Energy Inst. 89 (3) (2016) 366–372.

[12] R.K. Mohan, J. Sarojini, U. Rajak, T.N. Verma, Ü. Ağbulut, Alternative fuel production from waste plastics and their usability in light duty diesel engine: combustion, energy, and environmental analysis, Energy 265 (2023) 126140.

[13] A.A. Yusuf, et al., Effects of hybrid nanoparticle additives in n-butanol/waste plastic oil/diesel blends on combustion, particulate and gaseous emissions from diesel engine evaluated with entropy-weighted PROMETHEE II and TOPSIS: environmental and health risks of plastic wa, Energy Convers. Manag. 264 (2022) 115758.

[14] V. Sajith, C.B. Sobhan, G.P. Peterson, Experimental investigations on the effects of cerium oxide nanoparticle fuel additives on biodiesel, Adv. Mech. Eng. 2 (2010) 581407.

[15] V.D. Raju, S.R. Reddy, H. Venu, L. Subramani, M.E.M. Soudagar, Effect of nanoparticles in bio-oil on the performance, combustion and emission characteristics of a diesel engine, Liq. biofuels Fundam. Charact. Appl. (2021) 613–637.

[16] S. Jaikumar, S.K. Bhatti, V. Srinivas, R. Satyameher, S.B. Padal, D. Chandravathi, Combustion, vibration, and noise characteristics of direct injection VCR diesel engine fueled with Mesua ferrea oil methyl ester blends, Int. J. Ambient Energy 43 (1) (2022) 1569–1580.

[17] J. Lv, S. Wang, B. Meng, The effects of nano-additives added to diesel-biodiesel fuel blends on combustion and emission characteristics of diesel engine: a review, Energies 15 (3) (2022) 1032.

[18] M. Singh, P. Saini, D. Srivastava, S. Mishra, S.N. Ahmad, Effect of n-pentanol with novel water hyacinth biodiesel-diesel ternary blends on diesel engine performance and emission characteristics, Vietnam J. Chem. (2024).

[19] S. Nag, P. Sharma, A. Gupta, A. Dhar, Combustion, vibration and noise analysis of hydrogen-diesel dual fuelled engine, Fuel 241 (2019) 488–494.

[20] C. Dueso, et al., Performance and emissions of a diesel engine using sunflower biodiesel with a renewable antioxidant additive from bio-oil, Fuel 234 (2018) 276–285.

[21] S.K. Nagaraj, P. Ponnusamy, B.M. Nagarajan, Evaluation of emission in a diesel engine with neem and Pongamia (Karanja) mixed bio oil using 3-hole and 4-hole nozzle, Mater. Today Proc. 37 (2021) 2010–2013.

[22] M.S. Gad, B.M. Kamel, I.A. Badruddin, Improving the diesel engine performance, emissions and combustion characteristics using biodiesel with carbon nanomaterials, Fuel 288 (2021) 119665.

[23] M.K. Parida, P. Mohapatra, S.S. Patro, S. Dash, Effect of TiO2 nano-additive on performance and emission characteristics of direct injection compression ignition engine fueled with Karanja biodiesel blend, Energy Sources, part A Recover. Util. Environ. Eff. 46 (1) (2024) 7521–7530.

[24] J. Jayaraman, S. Reddy, Effects of injection pressure on performance & emission characteristics of CI engine using graphene oxide additive in bio-diesel blend, Mater. Today Proc. 44 (2021) 3716–3722.

[25] R.S. Gavhane, A.M. Kate, The effect of Sr-doped zinc oxide nanoadditives on the performance and emission parameters of a VCR engine powered by soybean biodiesel, Heat Transf. 51 (6) (2022) 5481–5496.

[26] M. Mourad, K.R.M. Mahmoud, E.-S.H. NourEldeen, Improving diesel engine performance and emissions characteristics fuelled with biodiesel, Fuel 302 (2021) 121097.

[27] P.M. Rastogi, A. Sharma, N. Kumar, Effect of CuO nanoparticles concentration on the performance and emission characteristics of the diesel engine running on jojoba (Simmondsia Chinensis) biodiesel, Fuel 286 (2021) 119358.

[28] B.J. Mitchell, et al., Engine blow-by with oxygenated fuels: a comparative study into cold and hot start operation, Energy 140 (2017) 612–624.

[29] F.M. Hossain, et al., Investigation of microalgae HTL fuel effects on diesel engine performance and exhaust emissions using surrogate fuels, Energy Convers. Manag. 152 (2017) 186–200.

[30] F. Hedayat, et al., Influence of oxygen content of the certain types of biodiesels on particulate oxidative potential, Sci. Total Environ. 545 (2016) 381–388.

[31] N. Jahnavi, K. Kanmani, P.S. Kumar, S. Varjani, Conversion of waste plastics into low emissive hydrocarbon fuel using catalyst produced from biowaste, Environ. Sci. Pollut. Res. 28 (2021) 63638–63645.

[32] C. Jin, et al., Effect of nanoparticles on diesel engines driven by biodiesel and its blends: a review of 10 years of research, Energy Convers. Manag. 291 (2023) 117276.

[33] P. Sharma, et al., Using response surface methodology approach for optimizing performance and emission parameters of diesel engine powered with ternary blend of Solketal-biodiesel-diesel, Sustain. Energy Technol. Assessments 52 (2022) 102343.

[34] P. Sharma, B.J. Bora, A review of modern machine learning techniques in the prediction of remaining useful life of lithium-ion batteries, Batteries 9 (1) (2022) 13.

[35] F. Okumuş, H.İ. Sönmez, A. Safa, C. Kaya, G. Kökkülünk, Gradient boosting machine for performance and emission investigation of diesel engine fueled with pyrolytic oil–biodiesel and 2-EHN additive, Sustain. Energy Fuels 7 (16) (2023) 4002–4018.

[36] N. Alper Tapan, R. Yıldırım, M. Erdem Günay, Analysis of past experimental data in literature to determine conditions for high performance in biodiesel production, Biofuels, Bioprod. Biorefining 10 (4) (2016) 422–434.

[37] A. Fayyazbakhsh, V. Pirouzfar, Comprehensive overview on diesel additives to reduce emissions, enhance fuel properties and improve engine performance, Renew. Sustain. Energy Rev. 74 (2017) 891–901.

[38] D. Damodharan, A.P. Sathiyagnanam, D. Rana, B.R. Kumar, S. Saravanan, Extraction and characterization of waste plastic oil (WPO) with the effect of n-butanol addition on the performance and emissions of a DI diesel engine fueled with WPO/diesel blends, Energy Convers. Manag. 131 (2017) 117–126.

[39] S. Kumar, G. Goga, Emission characteristics & performance analysis of a diesel engine fuelled with various alternative fuels–a review, Mater. Today Proc. (2023).

[40] S. Kumar, G. Goga, Review analysis on the performance & emission characteristics of a diesel engine fuelled with various gaseous & bio fuels, Mater. Today Proc. 80 (2023) 285–292.

[41] K. Ansari, G. Goga, R. Mohan, Utilization of food waste into ethanol and biodiesel, Mater. Today Proc. 65 (2022) 3596–3601.